LA-UR-13-20497
Approved for public release; distribution is unlimited.

Title: First-order beam dynamics and RF parameters for the PSR short-bunch ("pulse-stacking") mode

Author(s): Jason, Andrew J.

Intended for: Report

First-order beam dynamics and RF parameters for the PSR short-bunch ("pulse-stacking") mode

Andrew J. Jason
July 12, 2012

I. Introduction

Foreword

Here we mainly discuss the longitudinal ring beam dynamics and RF control for the bunching needed to maintain the short (a few nanoseconds) proton pulses required by the Weapons Neutron Research Center (WNR) for measurement of neutron cross sections and reaction dynamics, as specified in the recent upgrade proposal known as "Pulse Stacking." Single micropulses, each containing $6x10^8$ protons, are to be delivered to the Proton Storage Ring (PSR) from the LANSCE linac and successively overlaid in from 1 to 4 RF buckets per ring turn until a maximum number of particles in the bucket is achieved. This is distinct from the currently used long-pulse mode in which the bucket equals the ring circumference and a 201-MHz micropulse stream is injected at each turn to fill ¾ of the bucket to obtain pulses ~270 ns long.

That the short-bunch mode requires a buncher system to maintain a short pulse of a few nanoseconds is evident from kinematic considerations; with injection at a relative rms momentum spread of $\sim 6x10^{-4}$, during 100-μs accumulation, the first-turn beam will have broadened by 20-ns rms plus additional space-charge broadening if bunching is not implemented[1]. Longitudinal considerations are primarily dealt with in this note; in a previous memo [1], other aspects and a more general discussion of specific facility modifications to implement this mode are discussed. In particular, the required voltage of the bunching system is determined by the beam intensity as are, consequently, power, space considerations, and control requirements. The number of protons in each bunch is limited to $\sim 1x10^{11}$ per ns of bunch length from transverse-stability considerations. Tracking with available beam-dynamics programs may further define this quantity, but such analytical conclusions are usually close to limiting values.

The basic ground rules are 1 to 4 pulses stored in the ring with successive extractions at varying time separations ranging from 120 μs to 8.3 ms with substantial increase in beam current from present WNR operation (micropulse mode,) wherein a series of micropulses each containing $\sim 6x10^8$ protons is used during the 625-μs macropulse. The increase depends on the neutron energy of interest; for low energies the spacing between the micropulses in the micropulse mode must be large to prevent frame overlap, hence decreasing the total current, whereas the pulse-stacking mode provides a constant current. Additionally, the pulse length should be short enough not to dominate the resolution, balanced against a decreasing proton number/pulse with shorter pulse lengths. Further

[1] An experiment at the PSR was performed to assess a short bunch mode using the present 1st-harmonic buncher. Single bunches with up to $1.7x10^{11}$ particles and rms widths of 3-ns but with long tails were accomplished. See L. Rybarcyk, R. McCrady, and T. Spickermann, "A Test of Short-Bunch Stacking in the PSR," PSR Tech Note 06-001

discussion of the pulse structures and advantages to WNR is given in [1]. Repeating some of the information in [1] for reference, three modes are envisioned:

1) Accumulation of one pulse in the ring with immediate extraction during each macropulse, i.e. at 100 Hz;
2) four pulses in the ring with extraction ~every 2 ms, then immediate reload;
3) a new attenuated pulse injected every 120 μs with immediate extraction, thus 5 pulses/macropulse.

Three pulse lengths are dealt with here: 1.5, 5, and 10 ns that likely span the useful range of timings. At present, WNR favors the 10-ns pulse, but this study began with the shorter two pulse lengths, later modified to include the 10-ns option. Further study may exclude the 10-ns pulse as unviable, particularly in mode 2, because of the increased response time of the buncher cavity needed to support this pulse width. The three pulse widths are to be captured in ¾ of the phase width of the buckets produced by 503.125, 145.347 MHz and 72.673 MHz (or equivalently the 180th, 52nd, and 26th harmonic of the nominal ring frequency[2] of 2.795 MHz.) A choice of a single frequency is likely mandated to avoid the substantial complication of a further cavity. Bunch occupation numbers for the three respective frequencies are then nominally 1, 3, and $6x10^{11}$ protons/bunch.

It is tempting to find a scheme whereby successive buckets could be filled to ~double or triple the basic pulse width. Then the only possible buncher frequency would be 201 MHz to produce a basic pulse width of 3.75 ns as well as 6.25- and 11.25-ns pulses containing 2.5, 5, and $7.5x10^{11}$ protons, respectively. With the present (desirable) off-energy ring tune (see footnote 2) and the requirement that each injected micropulse contains $2x10^{8}$ protons, such a filling would marginally take the entire macropulse of 625 μs with no allowance for increasing the particles/pulse, unless the 201 MHz micropulse intensity were increased[3]. It would also introduce ripple in the delivered pulses.

In stating the given pulse lengths, beam spreading in transport (some 50 m) to the target has been neglected. With the predicted maximum momentum spread ~$4x10^{-3}$, a kinematic increase in pulse length of 0.2 ns is predicted (with negligible lengthening by space-charge effects.) This substantial transport distance to the target invokes consideration of RF manipulations in the transport line to shorten the pulse lengths. However, the transport distance is too short at the beam energy to achieve substantial changes in the pulse length without large voltages (estimated to be ~10 MV to 100 MV) on the low-frequency (less than half the ring-buncher frequency) cavity needed. The needed voltages are derived in Appendix A. Also note that bunch compression in the ring can be done by increasing the buncher voltage on a stored beam after storage, albeit with an attenuated

---

[2] Note that the ring is now operated at the 72.07th subharmonic of the linac frequency 201.25 MHz rather than the 72nd, to prevent overlap of micropulses in the long–pulse mode. This variation works out well for the micropulse mode since the injected pulse is walked along the bucket, excepting the 1.5-ns pulse that requires longer injection time and a more complex chopping since pulses from the regular pattern must be dropped as lying outside the RF bucket.

[3] A scheme has been proposed to further increase the WNR micropulse as well as to introduce RFQ compatibility by bunching the beam at 80 keV just after the ion source. See L. Rybarcyk, LINAC 06 and L. Rybarcyk and J. Lyles, PAC 07. The bunching per se would not help make the 201-MHz bucket concept feasible (a higher current ion source is needed,) but would be welcome for the three modes.

pulse. Such a technique is not discussed here, with major emphasis on obtaining a fixed-width bunch by injection techniques and maintaining RF control.

Parameters and symbol definitions

Relevant ring parameters are:

Radius R	14.4 m
Transition gamma γ_T	3.2
Slippage factor η	– 0.198
First harmonic current/10^{11} protons	0.0889 A -note that the Fourier component is 2x the average current
Fundamental frequency ω_0	2π x 2.795 MHz – harmonic number h=1
Proton velocity relative to the speed of light β	0.84
Lorentz factor γ	1.84
Ring period T	360 ns

Most of the symbols used extensively are listed:

Cavity voltage (not including transit time factor) V_c
Cavity decay constant $\alpha=\omega/2Q$ in sec^{-1}
Classical proton radius, r_p=1.5x10^{-18} m
Proton mass, m_p=938 MeV
Phase in cavity field ϕ in radians
Maximum bunch-length phase ϕ_m
Detuning phase ϕ_0
Number of particles in a bunch N
Eventual number of particles to be stored in a bunch N_0

Document contents

The document is organized as follows:

First, Beam dynamics is discussed in Sections II - VII

- Section I. Above, gives a brief summary of document scope. In particular, defines the three modes of operation and refers to reference [1] for details.
- Section II. A first-order calculation of transverse limitations on beam intensity is presented.
- Section III gives an overview of possible RF-cavity configurations and gives likely parameters that are used in subsequent calculations.
- Section IV summarizes older calculations on beam storage parameters to establish notation and formalism for further excursions into beam dynamics.
- Section V provides formalism for tracking beam longitudinal envelopes during changing particle number.
- Section VI utilizes the results of Section V to track beam envelopes during injection, providing a means to determine needed cavity voltages.

- Section VII gives results for needed cavity voltages and particularly notes that the static determinations of Section IV do not apply to an injected beam.

RF-confinement stability with the given dynamic parameters are discussed in Sections VIII – XV

- Section VIII calculates the Fourier components of the beam-current to be used in determining cavity response.
- Section IX shows how ring cavities must be tuned to achieve beam storage, in particular, with a minimum-power solution.
- Section X gives the conditions for RF stability.
- Section XI calculates instability damping time as a function of particle number and tuning angle, particularly noting that the minimum-power solution is stablest.
- Section XII gives numerical results for tuning parameters for the 4-bunch mode and a single-bunch mode.
- Section XIII offers an alternative to the minimum-power solution that eases cavity-tuning range with subsequent requirements on the RF generator power and phase.
- Section XIV gives details of stability parameters for modes 1 and 3, defined above.
- Section XV briefly comments on further aspects of stability and beam dynamics.
- Section XVI summarizes the note

The subsequent appendices give further detail to the main text and are therein referred to.

II. Transverse considerations

The first-order transverse limitation on the ring beam intensity arises from the space-charge tune shift toward an integer value from the nominal x and y tunes of 3.17 and 2.14. Known as the Laslett tune shift the tune shift from beam defocusing in a uniformly charged bunch of radius r is given as

$$\Delta\nu = -\frac{r_p R^2}{\gamma^3 \beta^2 r^2 \nu}\frac{N}{L}, \qquad 1)$$

where r_p is the classical proton radius $1.5\text{x}10^{-18}$ m, ν is the tune, R the ring radius 14.4 m, and N/L is the number of protons/m. Setting $\Delta\nu = -0.1$ and $r = 1$ cm a longitudinal particle density of $\sim 1\text{x}10^{11}$/ns is obtained. The same result is obtained for the PSR long-bunch mode with $2.5\text{x}10^{13}$ protons. In present operation, somewhat higher particle densities can be obtained, but with a larger r (a 1.6-cm bump). It is desirable to inject a smaller-radius beam in the short-bunch mode by bumping strategies to avoid foil interactions and losses during the long storage times contemplated. While the present specification is conservative, a factor of two increase in the given pulse intensities is not likely.

The real impedance of the ring is apparently low enough to avoid traditional transverse instabilities and should not occur with the lower short-pulse stored current (< 1 A as compared to ~15 A.) We have not gone through higher transverse-instability analyses for this exercise, particularly since the impedance of the ring is not available. The transverse-optics behavior of the ring has been well explored [2] and the low-order caveats appear to be entirely longitudinal as explored here. The transverse-injection process for the long-

and short-pulse modes remains the same so that little attention is likely needed to the ring optics except for increasing the bump magnets' rise and fall rate. Adding a horizontal bump may be propitious, but is not included in this proposal.

III. RF systems overview

Properties of the three cavity systems insofar as determined are listed.

503-MHz cavity

Substantial thought had gone into short-pulse bunching at the PSR inception. Although recent considerations indicate that the 1-ns-pulse-length requirement then in vogue is not optimum in a balance between intensity and neutron-energy resolution, we include this study as an option and as prototypical of longer pulse length. The parameters then specified included application of harmonic number 180 (503.125 MHz) to capture of single micropulses [3]. Instead of the originally specified 1-ns bunch (180° full phase width) we adopt a 1.5-ns bunch (270° width) to enhance stability. Stability requirements were to be met by fast (for injection and individual-bunch extraction) detuning of the cavity through a coupled auxiliary cavity that contained microwave ferrite (YIG, Trans-Tech G810, still the apparent best choice here) magnetically biased perpendicular to the cavity's RF field and above saturation to limit losses. Until this innovation, cavity tuning had universally been done with intrinsically slower ferrite arrangements magnetically biased along the cavity RF magnetic field, e.g., the PSR fundamental mode cavity and most synchrotrons. Perpendicular biasing (with field above the gyromagnetic resonance) using the appropriate ferrite results in faster response and lower losses. More recent applications of such tuning are sparsely evident [4] and a custom tuner can be made commercially [5], possibly advisable to avoid substantial development. At the demise of the short-bunch mode, a prototype system had been nearly completed but not tested although a model-tuning cavity performed well in prior tests. Further investigation of ferrite properties had been done in connection with synchrotron design for LAMPF II [6].

A drawing of the planned 503-MHz system is shown in Fig. 1 taken from [2] wherein further details can be obtained. Main cavity parameters are given for suggested operating conditions and with two cavities in the ring:

Total cavities voltage V_c	1.57 MV
Total shunt impedance R_s	43 MΩ
Unloaded Q	31000
Harmonic number h	180
2-cavity length (4 cells)	2 x 0.502 m
Transit-time factor	0.79
Total cavities' power at V_c=1.7 MV	105 kW
Unloaded cavity time constant (exponential)	19.6 μs

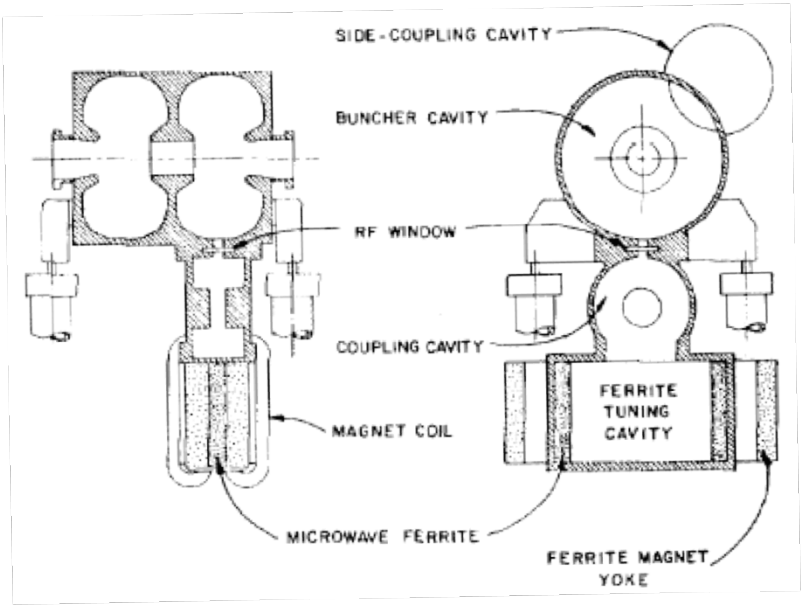

Fig. 1 . The PSR 503-MHz short-pulse buncher assembly showing the tuning arrangement. The two-cell cavity length in the figure is ~0.5 m and four such assemblies were envisioned in the ring.

The tuning cavity concept, prototypical of all our tuning provisions, also taken from [2] is shown in Fig. 2. The (exponential) cavity time constant is 3.5 μs, faster than the main cavity.

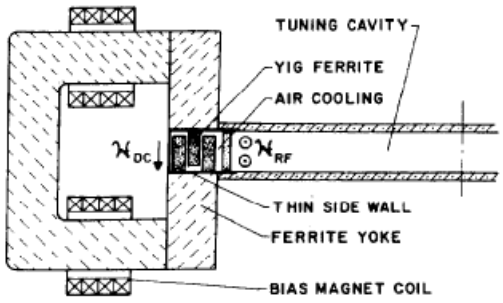

Fig. 2. Cross section of the ferrite-tuning cavity envisioned for the PSR short-bunch mode. The magnet gap is ~3.2 cm. A 1-kG field alters the tuner-cavity frequency by ~5 MHz for a 100- G variation with a then 100-kHz variation in the main-cavity frequency. Only a few-percent change in the tuning-cavity Q (~5000) with the magnetic-field tuning was noted since the ferrite is saturated with μ varying from ~3 to 5.

145 MHz cavity

A possible (145.34 MHz, harmonic number 52 and folded λ/2) cavity type is shown in Fig. 3. This frequency produces a 5-ns bunch. Its advantages include a lower bunching voltage with lower power requirements at higher intensities and use of only one cavity. Disadvantages include a narrowed stability range and a slower tuning rate and requirement of a larger tuner.

A suitable tuning cavity has not been designed but could follow the 503-MHz plan, i.e., addition of a coupled cavity. Cavity parameters are given

Cavity voltage V_c	0.56 MV
Cavity shunt impedance R_s	9.81 MΩ
Unloaded Q	20000
Harmonic number h	52
Transit-time factor	0.98
Cavity length ($\lambda/2$)	1.03 m
Cavity radius	25 cm
Cavity gap	20 cm
Aperture radius	6 cm
Power at V_c=0.52 MV	28.7 kW
Unloaded cavity time constant	44 μs

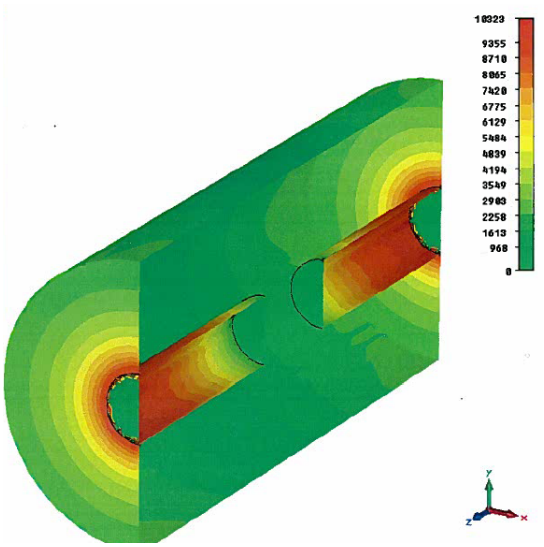

Fig. 3. Microwave Studio drawing of a possible 145 MHz cavity. Drawing and parameters are from Sergey Kurennoy. The distribution of surface currents is shown with scale in A/m for a gap voltage of 667 kV. An auxiliary tuning cavity is not shown.

73 MHz Cavity

We have not gone through the cavity design process for this frequency. However there are literature concepts that we can extrapolate from to form approximate parameters. Illustrations (Fig. 4) and parameters adapted from these literature articles are shown below.

Cavity voltage V_c	0.21 MV
Cavity shunt impedance R_s	4.4 MΩ
Unloaded Q	21000
Harmonic number h	26

Transit-time factor	0.98
Cavity length	2.6 m
Cavity radius	50 cm
Cavity gap	10 cm
Aperture radius	6 cm
Power at V_c=0.21 MV	10.6 kW
Unloaded cavity time constant	93 μs

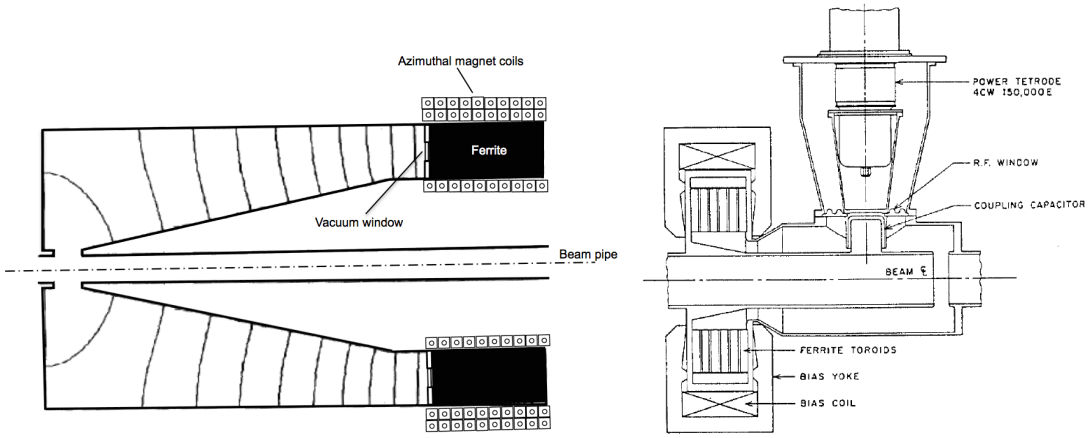

Fig. 4. Variants of possible 73-MHz cavities taken from literature. The left figure is adapted from [3], Early and Thiessen, while the right figure is directly from [6]. Cavity parameters above are extrapolated from [3]and may not be correct for a thorough design.

Remarks on RF system design

The cavity Q can be affected by design and should be minimized to provide the fastest response since beam parameters change rapidly and longitudinal-instability-damping becomes most favorable by a fastest response. Additionally, the shunt impedance should be minimized, a seemingly counter-intuitive requirement since the cavity power is thereby increased. However, power is modest and the tuning necessary to achieve maximum stability is minimized with the shunt impedance since the beam-induced voltage is least. Note that the PSR long-bunch mode operation does not require tuning, despite heavy beam loading, since means were taken to reduce the impedance seen by the beam (~10 Ω) with RF-source loading (~4kΩ) unchanged. The scheme used cannot be readily implemented with the short-bunch frequencies unless an unprecedentedly clever technique is devised.

IV. Capture calculations

We first use the formalism of R. Cooper [7] for the bucket size with additional comment. The results are analytical with inclusion of a space charge model and were originally used in specification of cavity parameters. There is substantial agreement with many observations for PSR performance. Stability is not included but will be discussed later. More detailed derivations for the formulae cited may be found in [7] but are sketched

here in a different parameterization for an appreciation of their assumptions and as a guide to further performance elaboration. However, as we will discuss later, the static conclusions of this formalism are not a good guide to an injection sequence. Nonetheless, the technique is of intrinsic and unique interest in obtaining a closed formalism incorporating much of the ring physics and we later use the results in formulating an injection scheme.

To proceed we note Cooper's space-charge model. Here we parameterize the motion in terms of RF phase, instead of the distance coordinate *z*. Note that expressing mass units in eV allows us to set $e=c=1$, hence $m_p c^2/e \rightarrow m_p$ in relations after 2). With this, all relations are nonetheless in MKS units after inserting r_p for the classical proton radius in meters. (The relations between the phase, distance, and time relative to the bunch center are given by $\phi = \frac{h}{R} z = -\frac{h\beta}{R} t$.) An approximate (and traditional) expression for the longitudinal electric field is

$$E_z = -\frac{ge}{4\pi\varepsilon_0 \gamma^2} \frac{\partial \lambda}{\partial z}, \qquad 2)$$

where λ is the particle number-density in *z* (here assumed parabolic to provide a uniform *z* field) and $g = 1 + 2\ln(b/a)$, the usual form factor for a transversely uniform beam of radius *a* and with pipe radius *b*. This dismissal of details of the transverse beam motion is common and is used in many tracking codes, e.g., identically so in ESME [8], since a full 6-D simulation is difficult.

This electric field *x* $2\pi R$ gives the voltage change V_s of a particle per unit ϕ in a trip around the ring due to space charge

$$V_s = \frac{3\pi g r_p m_p N h^2}{\gamma^2 R \phi_m^3} \qquad 3)$$

The zero-current equation of motion has then an added term proportional to ϕ, specifically

$$\frac{d^2\phi}{dt^2} = -\Omega^2 \sin\phi + \Omega_s^2 \phi, \qquad 4)$$

where Ω is the single particle synchrotron frequency

$$\Omega^2 = \frac{\omega_0^2 \eta h V_c}{2\pi\beta^2\gamma m_p}, \qquad 5)$$

and the contribution to the synchrotron motion from the bunch internal field is given by

$$\Omega_s^2 = \frac{\omega_0^2 \eta h V_s}{2\pi\beta^2\gamma m_p}. \qquad 6)$$

Integrating Eqn. 4) once and introducing the momentum spread as

$$\frac{d\phi}{dt} = -\omega_0 h \eta \frac{\delta p}{p} \qquad 7)$$

yields a potential [bracketed quantity in 8)] in which a particle moves, i.e.,

$$\left(\frac{\delta p}{p}\right)^2 + \frac{1}{\omega_0^2 h^2 \eta^2}\left[2\Omega^2(1-\cos\phi) + \Omega_s^2\phi^2\right] = \text{constant} \qquad 8)$$

This potential has local maxima symmetrically around $\phi=0$ and, for minimal containment, the phase at the maxima (turning points) ϕ must be equal to ϕ_m. Thus, a minimum buncher voltage is obtained proportional to the number of particles,

$$V_c \geq \frac{3\pi g r_p m N h^2}{\gamma^2 R \phi_m^2 \sin\phi_m}. \qquad 9)$$

Setting b=5 cm and a=1 cm, this may be evaluated for $\phi_m=3\pi/4$

$$V_{c\min} = 2.99\text{x}10^{-16} N h^2 \qquad 10)$$

or, for the frequencies 503, 145, and 73 MHz with 1, 3, and 6x10^{11} protons (in the single bunch,) $V_{c\,min}$=0.97, 0.24, and 0.12 MV, respectively.

Since 6) is a conservation rule, it may be taken equal to its expression at the turning points where $\delta p/p = 0$ to obtain a trajectory of the bucket bounding envelope,

$$\left(\frac{\delta p}{p}\right)^2 = \frac{2}{\omega_0^2 h^2 \eta^2}\left[\Omega^2(\cos\phi - \cos\phi_m) + \frac{\Omega_s^2}{2}\left(\phi^2 - \phi_m^2\right)\right] \qquad 11)$$

applicable only for $V_0 \geq V_{0min}$. A certain momentum spread (at ϕ=0) is associated with the minimum voltage and from 9) it is straightforward to show that this minimum spread is

$$\left(\frac{\delta p}{p}\right)_{\min}^2 = \frac{3 g r_p h N}{4\beta^2\gamma^3\eta R}\left[\frac{\frac{\phi_m}{2}\tan\frac{\phi_m}{2} - \left(\frac{\phi_m}{2}\right)^3}{\left(\frac{\phi_m}{2}\right)^3}\right] \qquad 12)$$

Evaluated at the stated particle populations $(\delta p/p)_{\min}$ is 0.25%, 0.23% and 0.23% for the three frequencies, respectively, about the same since we have scaled N approximately inversely with h. These latter quantities are of interest since a large intrinsic momentum spread may result in a too large beam from ring dispersion, while injection may lie outside the bucket with a small momentum spread.

It may be of interest to compare these predictions with PSR observations. The calculated minimum RF voltage (h=1, $\phi_m=3\pi/4$) for 4x10^{13} protons is 11.97 kV (not accounting for the transit time factor) and the minimum $\delta p/p$ is 0.37%. If the buncher voltage is raised to its (current) maximum of 16 kV, $\delta p/p$ becomes 0.48%.

Figure 5 shows the bounding trajectories Eqn. 11) at the minimum voltages for 1x10^{11} and 2x10^{11} particles in the bunch at h=180 and $\phi_m=3\pi/4$.

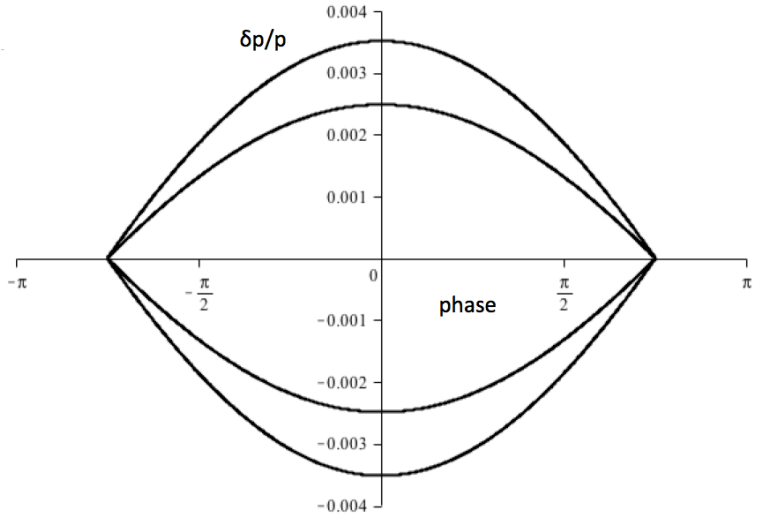

Fig. 5. Plot of bounding trajectories for the calculated (see Eqn. 10) minimal voltages to capture 1x10[11] (inner curve) and 2x10[11] protons for the 503 MHz case. The respective applied buncher voltages are 0.97 MV and 1.94 MV. The bucket extends over 0.38 m or 1.5 ns.

Plotted as a function of phase, the minimal buckets for the other two frequencies look virtually identical and, in the interest of brevity, are not shown.

In either case, the minimum momentum spread is above the nominal beam spread from the linac, allegedly ~0.0006 rms. Redistribution of the beam will occur due to the synchrotron motion that evolves more rapidly than the injection time (unlike the long-bunch mode.) Additionally, there exists a gratis painting along the phase axis from the present operation of the ring off the beam energy (see footnote 2.) Nonetheless, the final beam distribution will change with this painting and it may be well to consider the consequences with simulations.

V. Longitudinal tracking

Inspired by the above methods, a first-order algorithm for longitudinal particle tracking can be readily derived for the above model of space charge. For each turn of the ring, assuming a single cavity, the change in our variables is given by

$$\Delta\left(\frac{\delta p}{p}\right) = -\frac{V_c \sin\phi}{\beta^2\gamma\, m_p} + \frac{3\pi g r_p h^2 N}{\beta^2\gamma^3 R\,\phi_m^3}\phi \qquad 13)$$

$$\Delta\phi = -2\pi h\eta\frac{\delta p}{p} \qquad 14)$$

Although derivation of these two equations is relatively straightforward given the formalism of section II, their proofs are shown in Appendix B. It is well to again note that the beam distribution in phase is not self-consistently obtained, but as noted is assumed to be parabolic providing a linear space-charge term and a well-defined extent. A true tracking program would produce its own self-consistent distribution given an injection

distribution and may be more accurate (within statistics) but parameter dependencies are not then readily apparent.

A straightforward tracking program using 11) and 17) produces the results[4] in Figs. 6, 7, and 8 for voltages just above the minimum values. As would be expected identical axis intersections as in the previous section are found. A virtue of the tracking is that the space-charge-influenced synchrotron motion becomes apparent and for this reason we show the trajectories for all three cases.

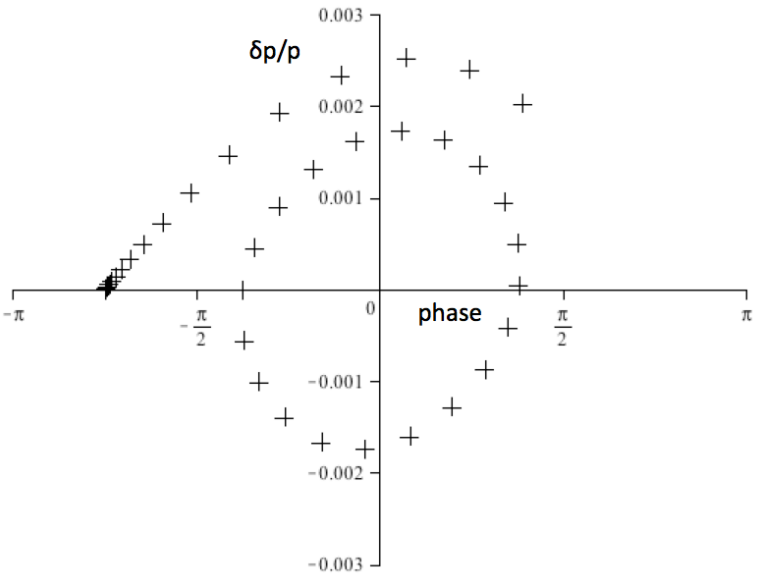

Fig. 6. Turn-by-turn tracking of synchrotron motion for the h=180, 1.5-ns pulse length, $1x10^{11}$ particles, and minimal-voltage. 20 turns are shown for the initial conditions $\delta p/p = 0$ with $\phi = -3\pi/4$ (outer curve) and $\phi = -3\pi/8$.

[4] The tilt in the trajectories envelope is from the phase change in motion around the ring and observation of each point just before buncher application. The tilt would be in the opposite direction if observed after the buncher. Such a tilt would be observed in an actual ring measurement depending on the measurement location.

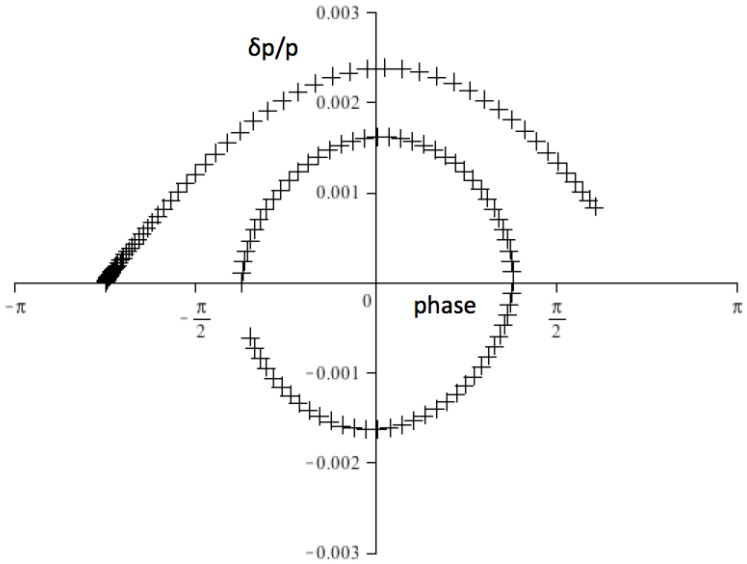

Fig. 7. Turn-by-turn tracking of synchrotron motion for h=52, 5-ns pulse length, $3x10^{11}$ particles and minimal voltage. 70 turns are shown for the initial conditions $\delta p/p = 0$ with $\phi = -3\pi/4$ (outer curve) and $\phi = -3\pi/8$.

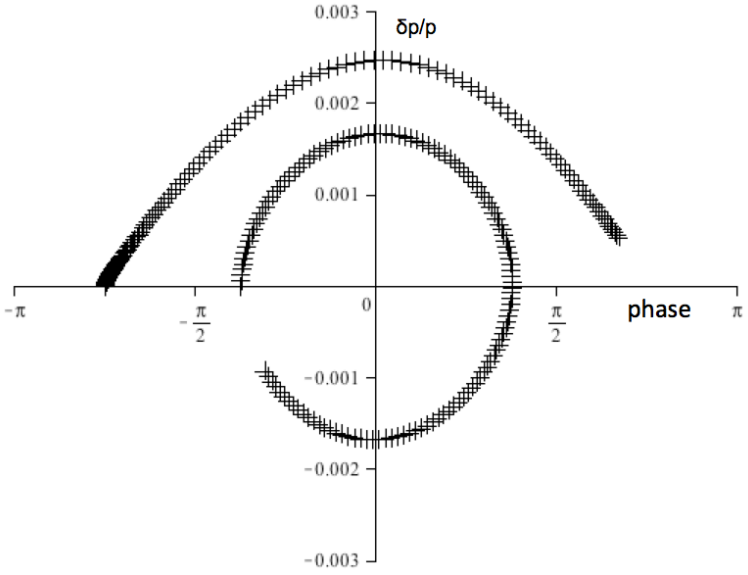

Fig. 8. Turn-by-turn tracking of synchrotron motion for h=26, 10-ns pulse length, $6x10^{11}$ particles and minimal voltage. 130 turns are shown for the initial conditions $\delta p/p = 0$ with $\phi = -3\pi/4$ (outer curve) and $\phi = -3\pi/8$.

In particular, increasing the particle number or lowering the voltage causes unstable motion, with the successive turns moving away from the bunch. Of course the synchrotron frequency increases with voltage as does the momentum spread. The monolithic space-charge model of Eqn. 2) has been augmented by addition of a $1/\phi$ field outside the presumed bunch as noted in Appendix C.

These three options seem to bracket the desirable set of options for pulse stacking. A further attractive option might be a 201.25 MHz (h=72, 3.75-ns bunch length) cavity that uses RF technology more familiar to LANSCE.

Thus a first-order tracking method has been established that will allow following a changing number of particles in the bunch, with the assumption that the bunch shape doesn't vary, a desired end result in beam accumulation. It is to be noted that we are not troubled by computational accuracy; with our 20-digit calculation the motion is stable for 10's of thousands of turns, far more than planned storage times (<3000 turns.)

VI. Bunch injection programming

Criteria for voltage programming during injection is quite different than the storage conditions noted in the last Sections. We seek a scheme for programming the cavity voltage as injection proceeds and then further maintaining conditions for stable storage. An arbitrary voltage program will lead to bunch compression or loss of particles from the designated phase-space area. It is difficult for the present formalism to track situations in which the bunch width changes, since the formalism assumes a bunch width ϕ_m. However, it is clear that if the voltage tracks the space charge forces too rapidly, the bunch will be compressed and particle loss may ensue. If the eventual storage voltage is used during injection, particle loss will occur. Accelerator experience confirms this, as does a simulation shown in Fig. 9 where the voltage for minimum storage is maintained throughout injection.

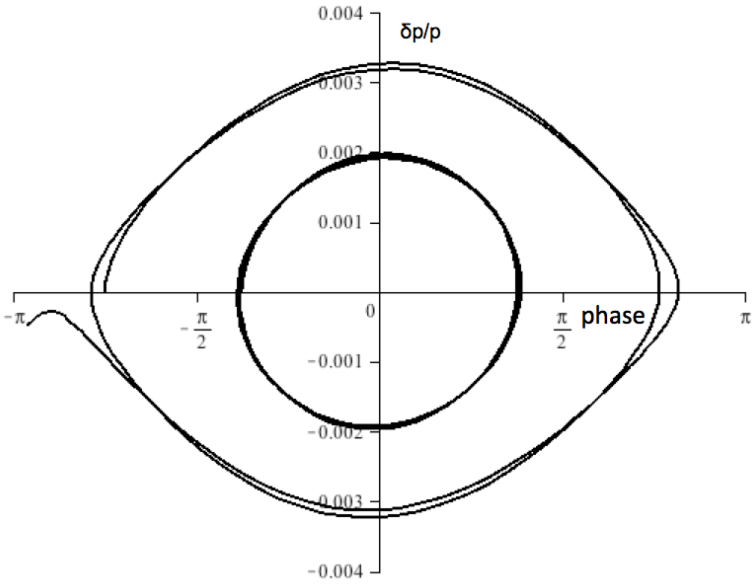

Fig. 9. Dynamic particle trajectories over 210 turns at h=52, V_c=0.25 MV with constant minimal voltage Eqn. 9) for 3x10^{11} protons injected over 500 turns. Particle loss from the extreme trajectory is seen at accumulation of 1.2x10^{11} protons. V_c must be increased by a factor of 3 to attain stability over 2000 turns, but very large momentum spreads are seen.

Again code exploration can be used to verify these assertions and tediously explore voltage programming, but we continue with an analytic approach to grasp the parameterization. In the present context, then search for a dynamic voltage sequence

versus particle number that maintains a constant bucket shape. This would occur if the buncher plus space-charge impulse were the same for each ring revolution. Because of the difference in forms of the kinematic and space charge terms in 13), this can only occur for one value of ϕ.

Consider application of voltage linear in the number of particles injected, i.e., for

$$N = N_0 t \qquad 15)$$

up to the maximum number of particles to be injected N_0 and t is the injection time from 0 to 1. Then the buncher voltage V_c is set at

$$V_c = V_1 + (V_2 - V_1)t \qquad 16)$$

where V_1 is an initial voltage and V_2 is the final voltage, attained and held when the number of particles is N_0, in general different from the storage voltage found above in Section III. Substituting in Eqn. 13) and setting the time dependent terms equal to zero, it is readily found that the required change in voltage during injection is given by

$$\Delta V \equiv V_2 - V_1 = \frac{3\pi g r_p h^2 m_p N_0}{\gamma^2 R \phi_m^3 \sin\phi}\phi \qquad 17)$$

The (remaining) time-independent part gives the magnitude of the momentum impulse per turn at a particular phase (same phase as Eqn. 17) of course.)

$$\Delta\left(\frac{\delta p}{p}\right) = -\frac{V_1 \sin\phi}{\beta^2 \gamma m_p} \qquad 18)$$

as might be anticipated from 13). There are two parameters to be chosen on the basis of stability, $\phi=\phi_c$ the phase at which the buncher kick is constant and V_1 the initial voltage at injection start. In general, by trial, pick $\phi_c=\pi/2$ and determine V_1 by bunch stability. Note that we are required to have a linear voltage rise by the fact that the number of stored particles is increased linearly with time.

As an example of how this works out, consider the 145-MHz case with injection (N_0) of $3\text{x}10^{11}$ particles. From 17) ΔV= 0.12 MV and setting V_1=0.4 MV for a storage voltage of 0.52 MV, kept constant at the end of injection. (Here we inject for 500 turns as would be required to accumulate the $3\text{x}10^{11}$ particles.) The injection history is shown in Fig. 8 as the change in momentum spread/turn. As advertised, the kick at $\phi=\pi/2$ remains constant. At the bunch ends ($\phi_m=3\pi/4$) the RF kick is smaller than at $\pi/2$ as noted in the figure. As injection proceeds the space-charge forces become larger and the bunch-ends kick smaller due to the balancing act between space-charge and RF fields at $\pi/2$.

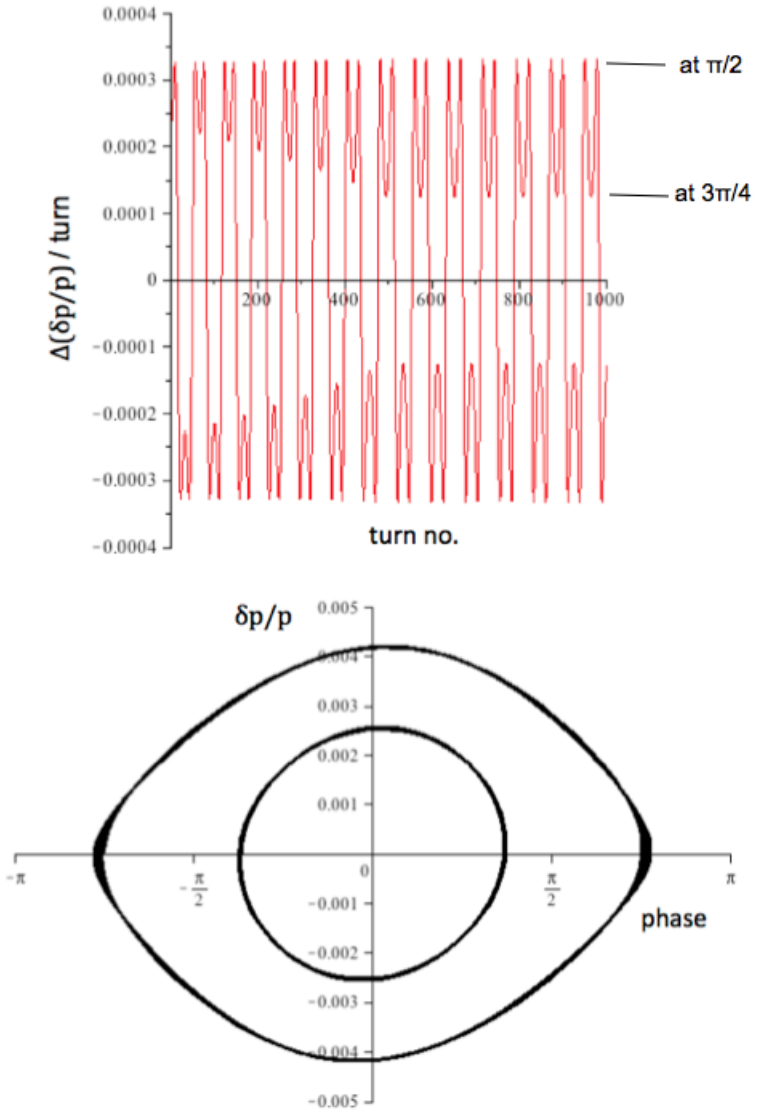

Fig. 10. Upper figure, particle-momentum kick versus turn number for conditions as noted in the text. Lower figure, phase space trajectories for a particle started at ϕ=-3π/4 (outer curve) and ϕ=-3π/8 followed for 2000 turns.

One intuitive way of finding a value for V_1 is, by noting that beam will not be confined without a net restoring force, we can determine the stability threshold implied by our model, assuming that bunch length is preserved throughout the injection process. Given a value for ϕ, we readily see that the kick 13) at ϕ_m is zero at injection end for

$$V_1 = \frac{3\pi g r_p h^2 m_p N_0 \left(\phi_m \sin\phi - \phi \sin\phi_m\right)}{\gamma^2 R \phi_m^3 \sin\phi \sin\phi_m}. \qquad 19)$$

This result, along with the value of ΔV Eqn. 15) is plotted in Fig. 11 for the 145 MHz case vs. ϕ=ϕ_c.

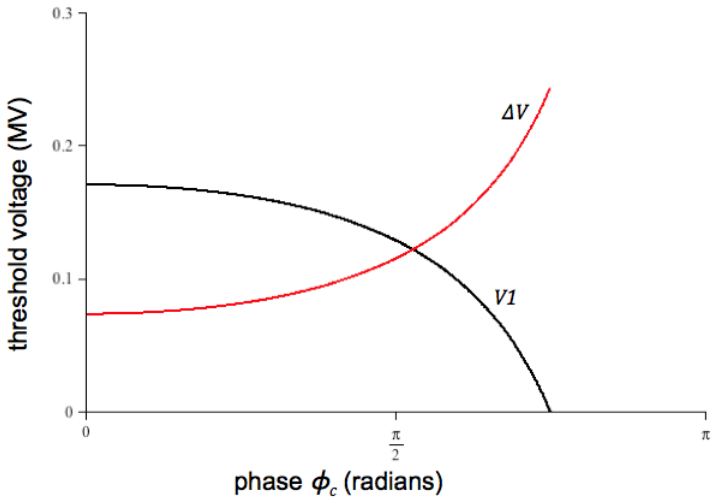

Fig. 11. Threshold voltages, as defined by 17] and 19] versus choice of optimum phase for bucket stabilization for the 145 MHz case with ϕ_m=3π/4.

For a given choice of ϕ_c the sum of the two voltages in Fig. 11, equals the minimal storage voltage, the result of Eqn. 9), hence containing the static case of Section III. This says little about the injection process and the stable value for V_1, to be determined by simulation.

VII. Results for voltage assignments

Results for the dynamic injection process are quite different than the quasi-static case noted in Section IV. There is a range of values for ϕ_c around π/2 that yield satisfactory bunch stability and tracking and such values minimize the eventual storage voltage. Using $\phi_c = \pi/2$, ΔV is determined by 15) and use of its calculated value produces a uniform kick at $\phi = \pi/2$ as seen in Fig. 10 for a wide range of V_1 values. Table I summarizes the results with notation as follows:

- ΔV is the change in cavity voltage seen by the beam during injection as calculated by Eqn. 17). All simulations discussed were done using this number.
- $V_{1\,min}$ is the voltage at the start of injection as calculated by Eqn. 19) that does not produce stable beam.
- $V_{1\,low}$ is the voltage at the start of injection at which motion is stable for more than 10,000 turns as determined by simulation. The onset of stability is sudden with V_1. Note that if the particles/bunch is decreased, the value of $V_{1\,low}$ will decrease.
- $V_{1\,good}$ is the voltage at the start of injection for which small bunch expansion is seen throughout injection and storage and at which our assumptions about a given bunch length are valid. Note that if the particles/bunch is decreased, the value of $V_{1\,good}$ will decrease.
- $V_{storage}$ gives the minimum voltage range to be maintained after injection, namely $V_{1\,min}+\Delta V$ to $V_{1\,good}+\Delta V$.
- δ p/p is the ± maximum beam-envelope momentum spread constant during injection storage voltage.

All voltages are peak voltages seen by the beam and do not include transit-time factors. Examples of the injection process are shown in Appendix E, inspection of which may help clarify the meaning of Table I.

Table I. RF system gap voltages in MV

	ΔV	$V_{1\,min}$	$V_{1\,low}$	$V_{1\,good}$	$V_{storage}$	$\delta p/p$ (%)
503 MHz	0.46	0.51	1.00	1.2	1.5 to 1.7	0.36 to 0.40
145 MHz	0.12	0.13	0.24	0.31	0.36 to 0.43	0.32 to 0.37
73 MHz	0.057	0.064	0.12	0.16	0.18 to 0.22	0.32 to 0.37
Long pulse $1x10^{14}$ protons	0.0057	0.0063	0.011	0.015	0.017 to 0.021	0.50 to 0.59

The following are observed in the simulations:

- Required voltages are independent of injection time.
- The onset of stability is sudden as V_1 is increased over a range of a few percent to $V_{1\,low}$.
- The momentum kick $\Delta(\delta p/p)$ at the bunch ends is greater than zero in the stable region as is seen in Appendix E.
- The bunch shape (orbits in longitudinal phase space) is maintained throughout injection and storage by the procedure in Section V and with $\phi_c \sim \pi/2$.
- The values of $V_{1\,low}$ are seen to be closely equal to the minimum voltage for storage predicted by 9).

The above injection and storage procedure is believed to closely represent the physics for the ring beam dynamics. Because of simplifications in modeling, experimentally determined quantities may depart from calculated values, but the ascribed range of voltages are likely to cover the performance values. Extended use of tracking codes may (perhaps) provide greater accuracy in performance assessment. However, the approximate agreement with the PSR parameters and provisional runs with the code ESME[5] are encouraging.

Only the basic first-order beam-dynamics instability has been so far discussed. Bunch-to-bunch interaction is yet to be assessed, as are resistive wall instabilities. However, performance of the ring with the long-bunch mode is encouraging here. If beam is well confined, the e-p instability seen by the PSR may not occur with the lower currents in the short-pulse mode. Further measures to preempt longitudinal instability are needed through beam interaction with the cavities as discussed below.

VIII. Beam spectra

The cavity system responds to the beam current as the Fourier component at its resonant frequency. The original assumption of the PSR study was that the (short) beam pulses were delta functions in which case all harmonics saw twice the dc current. That is, for

[5] Runs with ESME by Jeff Kolski showed particle loss ending within the range of V_1 given in Table I and substantial for voltages below $V_{1\,low}$.

N_0=10^{11} particles in a single pulse, the current was $2eN_0/T = 0.0889$ A for any harmonic, where T is the ring period. This is not a good approximation particularly for the longer pulses that we use.

Consistent with our space charge model, we use a parabolic distribution of beam current with full time width a,

$$I = \frac{6Q_0}{a^3}\left(\frac{a^2}{4} - t^2\right) \qquad 20)$$

where with the selected pulse width, h being the cavity harmonic number

$$a = \frac{3T}{4h} \qquad 21)$$

giving for the Fourier component of beam current at harmonic k

$$I_k = -\frac{32}{9}\frac{Q_0 h^2\left(3\pi k\cos\left(\frac{3\pi k}{4h}\right) - 4h\sin\left(\frac{3\pi k}{4h}\right)\right)}{\pi^3 k^3 T^2} \qquad 22)$$

Equation 22) is evaluated for 10^{11} particles in Fig. 12.

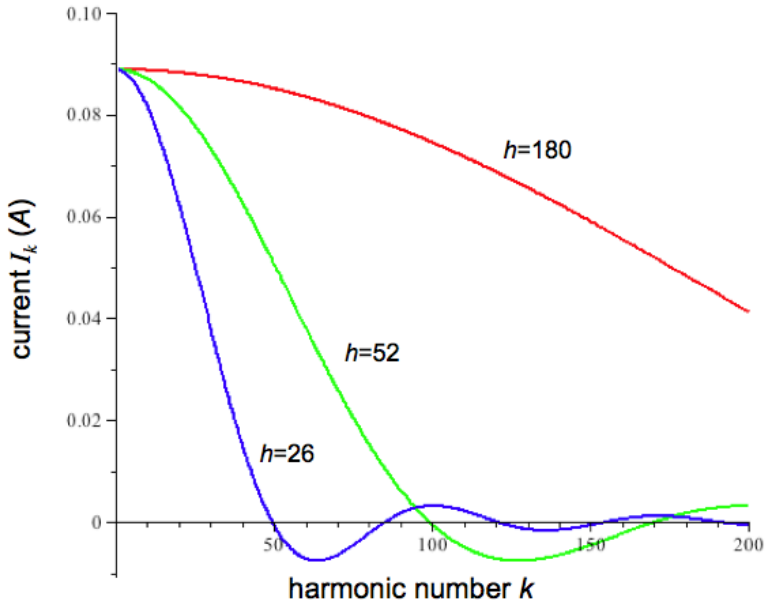

Fig. 12. Fourier component versus harmonic number for beam phase width of 3π/4 in the specified harmonic and charge of 10^{11} protons.

For the 3π/4 phase width and 10^{11} particles gives I_k=0.048 A for each of the three frequencies under consideration, or indeed for any harmonic k=h, nearly half of the delta function approximation. That is, either case gives 0.528 of the first harmonic current or 2 x 0.528 of the dc beam current. For the PSR original choice of a 1-ns pulse, I_{180}=0.069 A. Of course I_k is proportional to the number of particles in a bunch times the number of bunches.

Equation 15) gives information about the effects of co-existing cavities on the long- and short-pulse modes. With $4x10^{13}$ particles in the fundamental mode (17.7 A) the current seen at the three harmonics (180, 52, and 26) are 0.00059, 0.0071, and –0.00046 A, respectively[6]. The effect is some tens of kilovolts induced in the higher-frequency bare cavities and will affect the long pulse beam. Similarly, the presence of the short-pulse beam (per 10^{11} particles) will show up as 0.089 A in the first harmonic for either frequency, that would be negligible for a linear system, since the 2.8 MHz cavity has an impedance of ~10 Ω. However, the presence of ferrite in the cavity likely increases the impedance greatly at high frequencies. In either case, (difficult) active feedback or (unlikely) mechanical shorting may be considered to eliminate such effects.

Active feedback may be accomplished by insertion of a pickup in a cavity. One possibility is removal of the induced energy through a strongly coupled (but switchable) pickup, as is done in high-order-mode damping [9]. Alternatively, the pickup signal can initiate negative feedback in the cavity to zero its voltage. A worry is that such feedback may not be possible, i.e., controlling the cavity voltage around zero.

IX. Detuning the cavity

We follow the treatment and notation of references [10,13]. As with most such studies, an RLC circuit is used to model the system (shown to be a correct representation.) Relating the circuit to cavity parameters, the resulting differential equation is

$$\ddot{V} + 2\alpha\dot{V} + \omega_0^2 V = \alpha R_s \dot{I} \qquad 23)$$

where V is the cavity voltage, I the driver current (both beam and RF generator,) ω_0 the unperturbed resonance frequency of the cavity, and α, as defined above, is the decay constant for transient behavior (equal to $1.0x10^5$, $4.6x10^4$ and $2.2x10^4$ sec^{-1} for the 503-, 145-, and 73-MHz cavities, respectively using loaded Q values for a coupling constant =1.) Consider driving the cavity with frequency ω (or rather drive the cavity with ω_0 and detune the cavity to ω.) Using phasor notation, insert $exp(j\omega t)$ as the phase of the variables V, I with corresponding amplitudes ($j = \sqrt{-1}$.) The result looks complex, but neglecting small terms (assuming $\alpha << \omega$) the admittance is defined by the phasor quantities

$$\underset{\sim}{V_c} = \frac{R_s}{2\left(1 + j\frac{\delta\omega}{\alpha}\right)}\underset{\sim}{I} \equiv \frac{R_s}{2\left(1 + j\tan\phi_0\right)}\underset{\sim}{I}, \qquad 24)$$

additionally defining the relative phase ϕ_0 by driving the cavity off resonance, where $\delta\omega = \omega - \omega_0$, assuming the difference in the two frequencies to be relatively small. That is, in

[6] The sensitivity of I_k to distribution form is small for $k=h$ and other smooth distributions (than the assumed parabolic) with similar rms sizes, e.g., a Gaussian distribution. These values will be used in succeeding calculation. However, the effect of a first harmonic current, using the k of our cavities, can vary substantially with distribution width and shape. Hence the stated effect of the long pulse beam on the buncher cavities is not well defined.

phasor space the angle between the voltage and the current is ϕ_0 when the cavity is driven off resonance.

Set the current equal to the sum of the generator current (to the cavity) $-\underset{\sim}{I}_g$ and the beam current $-\underset{\sim}{I}_b$. Arbitrarily set the phase of the beam current along the real axis of a phasor diagram (that rotates counterclockwise with angular frequency ω) so that $\underset{\sim}{I}_b \rightarrow I_b$. Also note that for bunching the voltage must precede the beam bunch by 90°, hence $\underset{\sim}{V}_c \rightarrow -jV_c$ where the two quantities are now scalars.

Eqn. 24) now becomes

$$\underset{\sim}{I}_g = -\left(I_b + \frac{2V_c}{R_s}\tan\phi_0 \right) + j\frac{2V_c}{R_s} \qquad 25)$$

This is the condition for bunching established by the choice of phase for $\underset{\sim}{V}_c$. Not that we *a priori* have to, but power can be minimized and the cavity matched to the generator (no reflection to the isolator if the transmission line impedance is matched to the cavity) for

$$\tan\phi_0 = -\frac{I_b R_s}{2V_c} \qquad 26)$$

thus setting the phase of the generator current lagging the beam current by 90° (remaining term in Eqn. 18.) The phasor diagram now looks like Fig. 13. The diagram makes clear the need for cavity tuning[7]. The generator power is just sufficient to energize the cavity since the beam is not accelerated.

If the condition 26) is not maintained, the generator current must be increased to maintain bunching and will have a real component. This changes the phase angle between $\underset{\sim}{I}_c$ and $\underset{\sim}{V}_c$, a potentially useful possibility as shall be discussed in Section XII. The cavity power remains the same V_c^2/R_s, with the excess power reflected to the isolator. Of course, the RF generator must produce the excess power to be dumped in a load. For all of our cases the beam current is substantially greater than the generator current at maximum beam.

---

7 That cavity detuning is necessary (as well as difficult) is demonstrated by the SNS struggle to prevent loss from their ring bunch (see Y. Zhang, et al., "Simulation study and initial test of the SNS ring RF system," Proceedings of PAC 07; some details of their control system are included.) The SNS has chosen not to build in a low-impedance shunt to their cavity as in the PSR and so must control the beam/RF phase as indicated here.

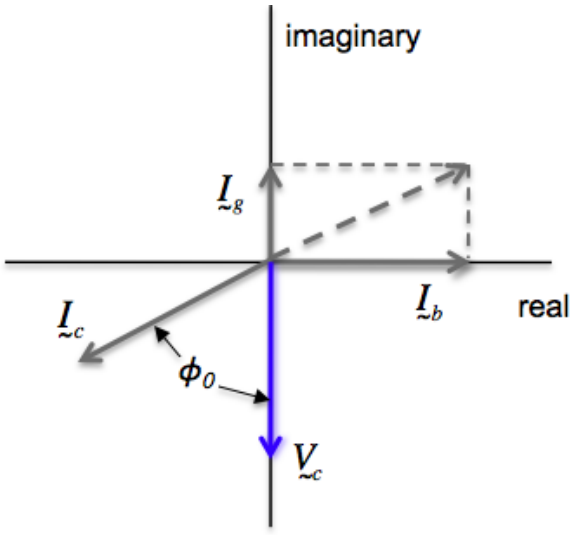

Fig. 13. Phasor diagram for minimum generator current. Note that the cavity current I_c is opposite the sum of the beam and generator currents, a straightforward consequence of the sign convention adopted for the RLC circuit.

X. First-order longitudinal stability

The lowest-order (dipole) longitudinal instability, known as the Robinson instability, was stated most lucidly by Cooper and Morton [10] in direct application to the PSR short-bunch mode. We draw heavily on their treatment but extend their conclusions and evaluate for our parameters.

The theory of the Robinson instability stems from perturbations to a particular steady state condition. The variables to be perturbed (for a given generator voltage and phase) are:

- the beam centroid phase (for a given generator voltage and phase)
- the beam-centroid energy
- the cavity-voltage phase
- the cavity voltage

The relation between the time derivative of these quantities and their values as well as other parameters can be derived from the phasor diagram Fig. 13. For details see references in [10].

The totality of these perturbations yields a set of coupled equations that have a range of solutions with time dependence $\exp(\gamma+j\omega t)$. Picking out the solutions for which damping occurs, $\gamma < 0$, the condition on the phase is the condition derived by Robinson.

$$\sin 2\phi_0 > -\frac{4V_c}{I_b R_s} \qquad 27)$$

with the additional constraint that $\tan \phi_0 < 0$ placing ϕ_0 in the second quadrant, 0 to $-\pi/2$. There are two regions of such solutions extending from the ends of the interval as shown in Fig. 14.

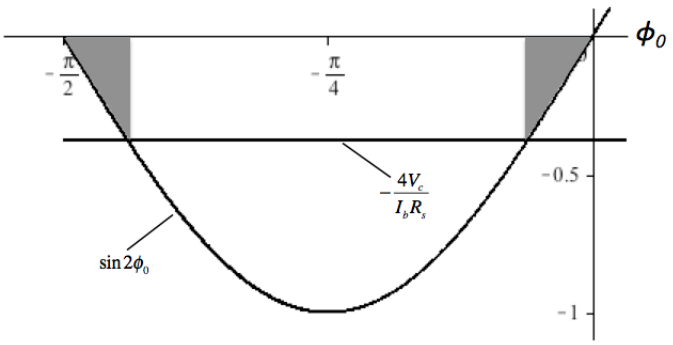

Fig. 14. Regions of longitudinal stability (shaded areas) for the cavity system as per Eqn. 27).

To interpret this diagram let $x = 4V_c/I_b R_s$, the negative of the right-hand side of Eqn. 27). If $x > 1$, corresponding to a low current or high buncher voltage, the motion is stable for any value of ϕ_0 between 0 and $-\pi/2$. For the minimal generator current case 26), it is straightforward to show that ϕ_0 lies in the left shaded area. These latter two assertions will be more evident in evaluation of the damping time in Section XI. If the generator current is not minimized, the restriction 26) need not be met but 27) must be. This requirement is analogous to restrictions on a linac or an accelerating ring where the beam center must be located on the time-rising side of the RF voltage, thus negative phases are needed. At our high currents, $x<1$, the beam drives the cavities and phase slippages must be corrected by the generator.

The offhand conclusion is that the cavity must be rapidly tuned to match the beam time structure and to the extent depending on the voltage program. Injecting particles occurs over 120 to 360 μs during which time the phase and voltage amplitudes must be varied in a program to match the storage conditions. Even more severe, when each pulse is extracted, the retuning of the system must occur very rapidly to accommodate the change in I_b and stability is to be determined for a finite tuning time.

It is noted that for the PSR long-bunch mode, with 4×10^{13} protons, the motion is always stable according to 27) and the detuning angle for minimum power is only ~2°, implying a frequency shift of ~350 Hz.

XI. Damping time

The theory of the Robinson instability stems from perturbations to a particular steady state condition. The variables to be perturbed (for a given generator voltage and phase) are:

- the beam-centroid phase (for a given RF-generator voltage and phase)
- the beam-centroid energy
- the cavity-voltage phase
- the cavity voltage

The relation between the time derivative of these quantities and their values as well as other parameters can be derived from the phasor diagram Fig. 13. For details see references [10]. Letting the time dependence of the quantities be $\exp(\gamma t)$, a set of four

coupled equations is obtained, linear in the variables. Requiring that the determinant of the variables' coefficients vanish gives

$$\gamma^4 + 2\alpha\gamma^3 + \left[\alpha^2\left(1+\tan^2\phi_0\right)+\omega_s^2\right]\gamma^2 + 2\alpha\omega_s^2\gamma + \alpha^2\omega_s^2\left(1+\tan^2\phi_0 + \frac{I_b R_s \tan\phi_0}{2V_c}\right) = 0 \quad 28)$$

where ω_s is the synchrotron frequency $\omega_0\sqrt{\eta h V_c / 2\pi m_p \gamma\beta^2}$. (That the synchrotron frequency enters notationally into the results does not mean that space charge need be taken into account; the derivation physics contains only the longitudinal centroid as appropriate for the Robinson instability.)

The quartic equation looks formidable, but is numerically solvable. Divide through by α^4 and let the quartic variable be

$$z = \frac{\gamma}{\alpha} \quad 29)$$

thus comparing the decay constant to the cavity time constant α as well as simplifying the computation.

To understand the ensuing results, first note that if the beam current is zero, the four equations are decoupled into two sets with solutions of the resulting quadratic equations in two conjugate pairs

$$\begin{aligned} z_{1,2} &= -1 \pm j\tan\phi_0 \\ z_{3,4} &= \pm j\frac{\omega_s}{\alpha} \end{aligned} \quad 30)$$

As the beam current is turned on, these solutions to 28) will evolve into stability criterion depending on selection of the roots and the sign of the root real part. Note also that for the minimum power solution Eqn. 26) the bracketed part of the last term in 28) becomes 1 with the remainder of the bracket reversing sign as the phase or current is changed. Here the expected solution discontinuity will be seen as the most stable operating point for our parameters, though not so in general.

Solutions to 28) were obtained (tediously) by the method of Ferrari [11]. The physically meaningful of the four solutions is determined by the Routh-Hurwitz criterion [12] applied to the coefficients of 28) that determines Eqn. 27), although the relevant solution is obvious by inspection. This selection corresponding to one of the first set of solutions in 30) is shown in Figs. 15 and 16.

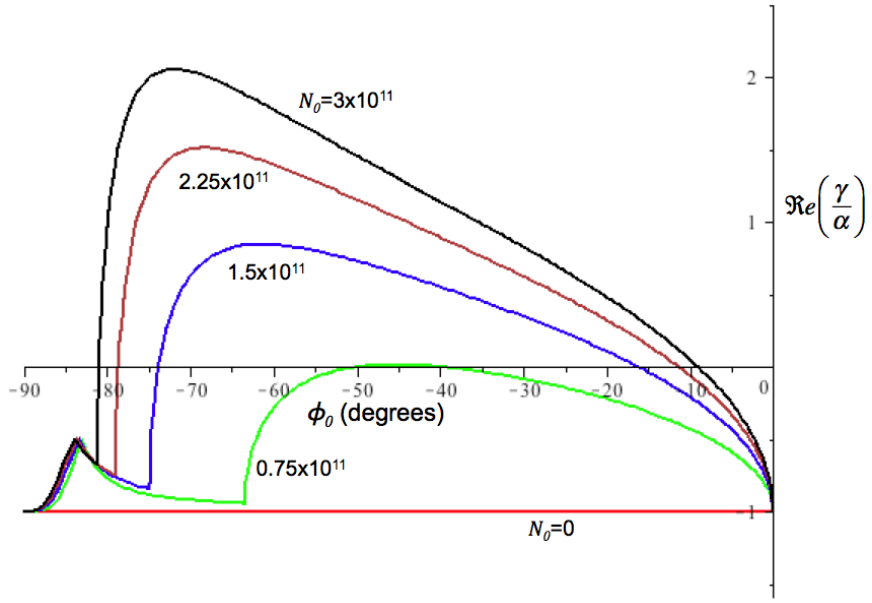

Fig. 15. For the 145 MHz case, shown is the real part of Eqn. 28) root versus tuning phase as a function of particles/bunch that shows RF system stability. Evolution from the zero-beam case ($z_{1,2}$ in Eqn. 30) is evident; with no particles the ordinate =-1. The zero crossings correspond to the prediction of Eqn. 27). The (lower) discontinuities in the traces' derivative correspond to the minimum generator-power settings 26), while the significance of the cusp is unexplained.

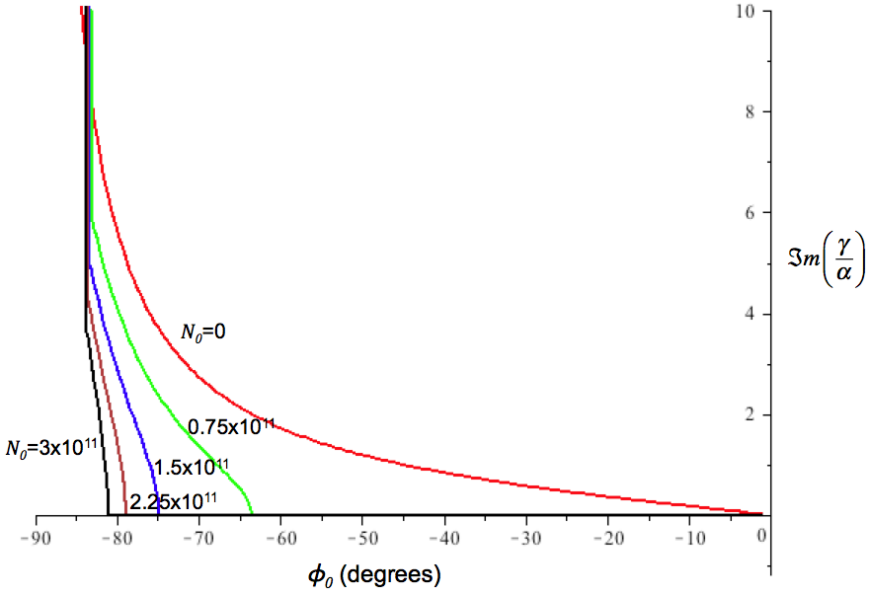

Fig. 16. For the 145 MHz case, the imaginary part of Eqn. 28) root versus tuning phase as a function of particles/bunch. Evolution from the zero-beam case ($z_{1,2}$ in Eqn. 30) is evident; the zero particle case is identically tanϕ_0. Here the imaginary part of the solutions is zero up to the minimum-power phase defining the region of critical damping. The discontinuities in the traces at ~ –85° correspond to the cusp in Fig. 15.

In these plots the buncher voltage is $V_c=V_{1\,good}+\Delta V\,N/N_0$, where N gives the particles/bunch. This specifies the voltage required for beam dynamics of any number of bunches. However, the total current in the ring is the relevant parameter and is set for four bunches, i.e., I_b in Eqns. 25) to 27) is 4 times the Fourier component of the current in a single bunch. Solutions outside the fourth quadrant are non-physical as is the other solution to $z_{1,2}$ and the solutions $z_{3,4}$. The solutions for the 503- and 73-MHz case are qualitatively the same as the 145 MHz case shown, but may be of interest to view in Appendix F. All plots may be compared with the numbers in Tables II and III below.

The salient conclusions here are

1. The damping of the instability is not faster than the cavity relaxation rate despite assertions of certain literature formulae. Assuming matched coupling between the RF generator and cavity, these time constants are 9.8, 21, and 46 μs, respectively for the three frequencies.
2. The fastest damping occurs at the phase for minimum power. Hence, with the heretofore results it seems counterproductive to move substantially further (increasing $-\phi_0$) into the stable region as had been suggested.
3. The imaginary part of the (alleged) physical solution is zero below the minimum-power phase, indicating critical damping (or pure exponential rise for $\Re\mathrm{e}(\gamma) >0$) of the instability.
4. The salient parameters in increasing areas of stability are the shunt impedance R_s (minimize) and the cavity Q (maximize.) Note however, that the solutions shown are yet a function of Q, i.e., through terms with ω_s/α in the reduction of 28).

XII. Results with minimal generator power

To minimize power from the generator, it would seem desirable to maintain relation 26) and thus eliminate reflected power. However, there are some possible reasons to violate this injunction as will be discussed later. In this Section Eqn. 26) is assumed. As mentioned, the stability criterion is automatically fulfilled and the instability is best damped if 26) is followed. Only a scattering of examples will be presented, but the effect of variations will be apparent. In each case assume two (there were four in the original proposal) 503-MHz cavities, one 145-MHz cavity, and one 73-MHz cavity. There may not be space in the ring for four RF stations.

It is evident that a linear rise in voltage $V_c=V_1+\Delta V\,N/N_0$ and adjusting ΔV by setting ϕ_c near $\pi/2$ in 17) produces a stable bunch shape and minimizes cavity voltages, according to the formalism presented. The "best" value for V_1 is determined by simulation although particle loss is not seen for somewhat lower voltages as discussed above. Results are accordingly presented for the voltages

$$V_{503}=1.2+4.6\text{x}10^{-12}\,N \text{ MeV for } 1\text{x}10^{11} \text{ particles}$$
$$V_{145}=0.31+4.0\text{x}10^{-13}\,N \text{ MeV for } 3\text{x}10^{11} \text{ particles} \qquad 31)$$
$$V_{73}=0.15+9.6\text{x}10^{-14}\,N \text{ MeV for } 6\text{x}10^{11} \text{ particles}$$

Table II shows RF-parameter results for 4 pulses in the ring. I_b is the Fourier component of the total beam current. Here the detuning frequency is calculated from the definition 24) for the minimum power phase 26) using the stated cavity Qs. The cavity powers (at

full voltage) were calculated using the given transit-time factors, but these are not included in the cavity voltages. Blanks in the stability tuning angle (5th column) indicate that the sine of column 4>1.

Table II. RF system parameters for 4 pulses in the ring

protons/pulse	I_b (A)	V_c (MV)	$-\frac{4V_c}{I_b R_s}$	stability ϕ_0 (deg)	min pow ϕ_0 (deg)	detun freq (kHz)	P_{cav} (kW)
503 MHz	Rs=43	4 pulses	2 cavities				
0	0	1.20	<-1	-	0	0.0	54.3
2.5E+10	0.05	1.32	-2.61	-	-37.5	-12.5	65.3
5.0E+10	0.09	1.43	-1.42	-	-54.7	-22.9	77.2
7.5E+10	0.14	1.55	-1.02	-	-63.0	-31.8	90.1
1.0E+11	0.19	1.66	-0.82	-62.3	-67.6	-39.5	104.0
2.0E+11	0.38	2.12	-0.53	-74.2	-75.3	-61.8	169.6
145 MHz	Rs=9.8	4 pulses	1 cavity				
0	0	0.31	<-1	-	0	0	10.2
7.50E+10	0.14	0.34	-0.99	-49.9	-63.8	-14.8	12.3
1.50E+11	0.28	0.37	-0.54	-73.8	-75.0	-27.1	14.5
2.25E+11	0.42	0.40	-0.39	-78.6	-79.1	-37.6	17.0
3.00E+11	0.56	0.43	-0.31	-80.9	-81.1	-46.7	19.6
6.00E+11	1.13	0.55	-0.20	-84.3	-84.3	-73.0	32.1
73 MHz	Rs=4.4	4pulses	1 cavity				
0	0	0.16	<-1	-	0	0	6.1
1.50E+11	0.28	0.17	-0.56	-72.9	-74.3	-12.1	7.2
3.00E+11	0.56	0.19	-0.30	-81.1	-81.3	-22.3	8.4
4.50E+11	0.84	0.20	-0.22	-83.7	-83.8	-31.2	9.8
6.00E+11	1.13	0.22	-0.18	-84.9	-85.0	-38.8	11.2
1.20E+12	2.25	0.27	-0.11	-86.8	-86.8	-61.4	17.9

Similarly, the results for a single pulse in the ring are shown in Table III.

Table III. RF system parameters for 1 pulse in the ring

protons/pulse	I_b (A)	V_c (MV)	$-\frac{4V_c}{I_b R_s}$	stability ϕ_0 (deg)	min pow ϕ_0 (deg)	detun freq (kHz)	P_{cav} (kW)
503 MHz	R_s=43	1 pulse	2 cavities				
0	0	1.20	<-1	-	0	0.0	54.3
2.5E+10	0.012	1.32	-10.43	-	-10.9	-3.1	65.3
5.0E+10	0.023	1.43	-5.67	-	-19.4	-5.7	77.2
7.5E+10	0.035	1.55	-4.08	-	-26.1	-8.0	90.1
1.0E+11	0.047	1.66	-3.29	-	-31.3	-9.9	104.0
2.0E+11	0.094	2.12	-2.10	-	-43.6	-15.5	169.6

145 MHz	Rs=9.8	1 pulse	1 cavity				
0	0	0.31	<-1	-	0	0	10.2
7.50E+10	0.035	0.34	-3.94	-	-26.9	-4	12.3
1.50E+11	0.070	0.37	-2.15	-	-43.0	-7	14.5
2.25E+11	0.11	0.40	-1.55	-	-52.3	-9	17.0
3.00E+11	0.14	0.43	-1.25	-	-58.1	-12	19.6
6.00E+11	0.28	0.55	-0.80	-63.6	-68.3	-18	32.1
72 MHz	R_s=4.4	1 pulse	1 cavity				
0	0	0.16	<-1	-	0	0	6.1
1.50E+11	0.070	0.17	-2.25	-	-41.6	-3.0	7.2
3.00E+11	0.14	0.19	-1.22	-	-58.7	-5.6	8.4
4.50E+11	0.21	0.20	-0.87	-59.5	-66.4	-7.8	9.8
6.00E+11	0.28	0.22	-0.70	-67.7	-70.7	-9.7	11.2
1.20E+12	0.56	0.27	-0.44	-76.8	-77.5	-15.3	17.9

The voltages cited are considered nominal, but higher voltages should be provisioned in actual design to enhance stability, consistent with allowable momentum spread.

XIII. Remove restrictions on generator power to decrease tuning range

It is possible to restrict the cavity tuning range by allowing the forward generator current to increase above its minimal value. This may be desirable in reducing the tuning section range and power. It is then necessary to vary the generator phase (relative to the beam current) from 90° to a value such that the cavity voltage remains constant and orthogonal to the beam current on a phasor diagram. This situation is shown in Fig. 17.

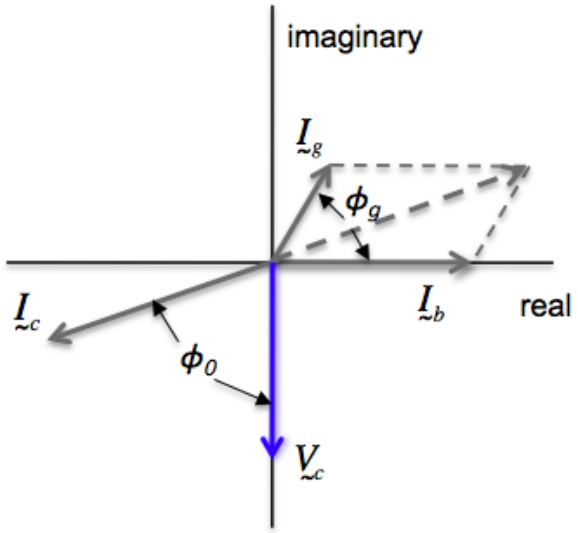

Fig. 17. Phasor diagram for the (controlled) RF system when the generator current is no longer minimized.

As the beam current changes during injection, the minimal phase (Eqn. 27) starts from zero and increases with the current. We consider adjusting both the generator current I_g and phase ϕ_g so that the cavity voltage is correct and the sweep of ϕ_0 is reduced,

appropriate to the constraints of Eqn. 27 and perhaps Eqn. 26). The price is power reflected from the cavity and lost in the isolator as well as more complex tuning.

Calculation of these quantities for a transmission line matched to the cavity (unity coupling constant) is straightforward and has been done in all generality for a given matching in [13]. Assuming this matching the following relations are obtained:

$$P_F = \frac{V_c^2}{R_s}\left[1+\frac{1}{4}\left(\frac{I_b R_s}{2V_c}+\tan\phi_0\right)^2\right] \qquad 31)$$

$$\tan\phi_g = -\frac{2}{\frac{I_b R_s}{2V_c}+\tan\phi_0} \qquad 32)$$

where P_F is the forward power of the generator. For the matched condition 19) our conditions in the previous Section are fulfilled with the disappearance of the denominator in Eqn. 23), i.e., $\phi_g=\pi/2$, and the forward power $P_F=V_c^2/R_s$.

Since, to our approximations, the system behavior is independent of time as long as the RF programming can be followed, characterize the sequence of events as

$$n = \frac{N}{N_0} \qquad 33)$$

where N_0 is the maximum number of protons injected, $1\text{x}10^{11}$, $3\text{x}10^{11}$, and $6\text{x}10^{11}$ particles, for the frequencies cases, respectively. Consider a linear voltage ramp as was done in Tables II and III,

$$V_c = V_1 + n\Delta V \qquad 34)$$

To characterize the tuning, vary $\tan\phi_0$ linearly from some initial value to the maximum of the minimum-power value $\tan\phi_{\max} = -\frac{I_{b\max}R_s}{2V_{\max}}$ (with V_{max} equal to the final value of V_c, $V_{\max} = V_1 + \Delta V$) as seen from 26), i.e.,

$$\tan\phi_0 = \left[n+(1-n)\kappa\right]\tan\phi_{\max} \qquad 35)$$

so that, when $\kappa = 0$, the tangent of the detuning angle is directly proportional to n and when $\kappa=1$ the detuning equals ϕ_{max} throughout changes in n. This is acceptable as long as $\tan\phi_0$ is within the stable region, Eqn. 27). This variation with n produces more-digestible results than other power laws. We can also add an angle to ϕ_{max}, but that has proven ineffective.

145 MHz case

Following the above prescription 34) and 35), there are many variations to explore that are not all described in this space. A reasonable solution for 145 MHz with $3\text{x}10^{11}$ ppp and 4 pulses is found for κ=0.5 with a –24 kHz tuning frequency change during injection (about half the value needed for the minimal power case) and a generator forward power

of initially 36 kW decreasing to the nominal value of 20 kW at injection end, to be maintained for storage. The final tuning angle equals the minimum-power tune. Results for the 145 MHz case are shown in Figs. 18 and 19.

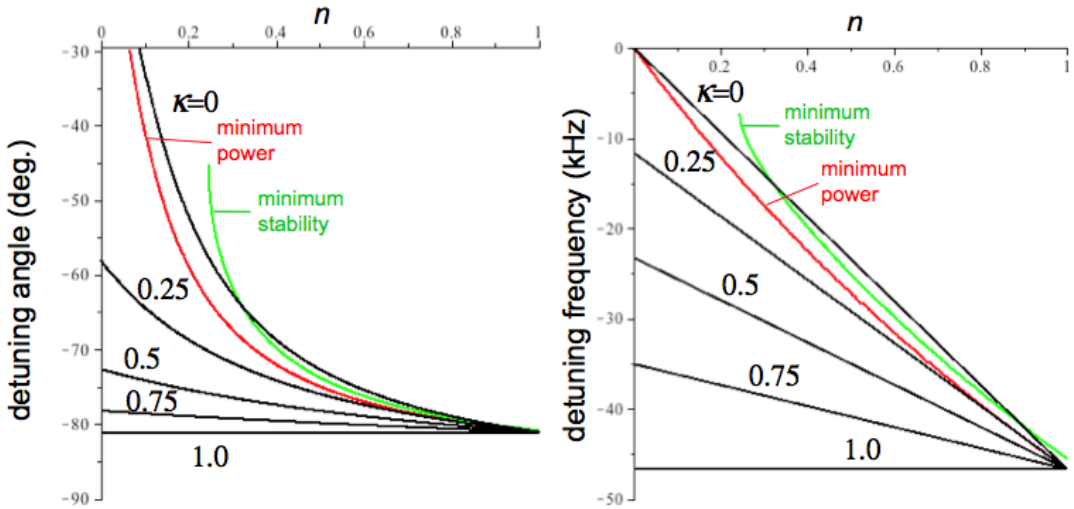

Fig. 18. Exemplary plots at 145 MHz of the tuning angle (left) and frequency (right) versus the relative number of particles injected as a function of the tuning parameter κ using relations 34) and 35) for the tuning program. There are 4 pulses in the ring and N_0=3x10^{11} It is evident that κ=0 is not a viable solution.

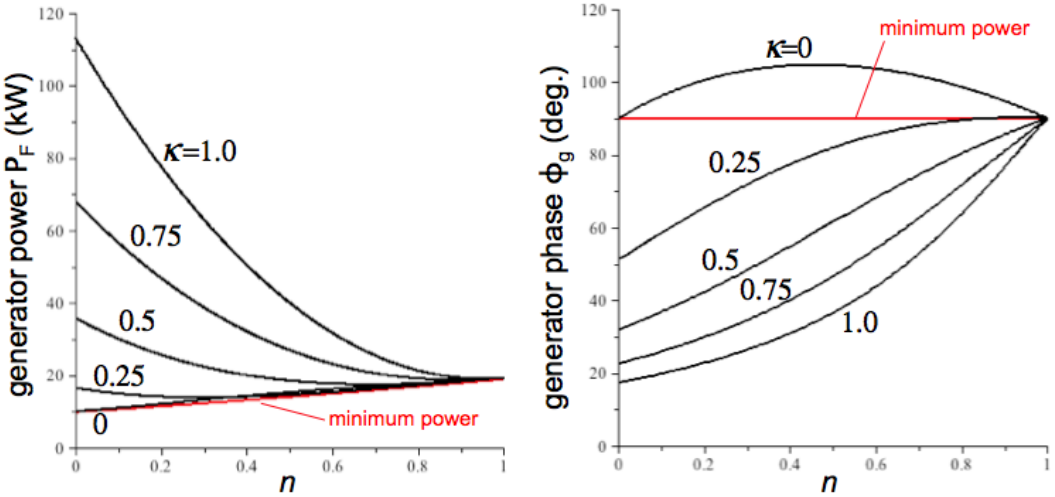

Fig. 19. Plots at 145 MHz of the generator power (left) and phase (right) versus the relative number of particles injected as a function of the tuning parameter κ using relations 34) and 35) for the tuning program.

The tradeoffs are apparent:

- The detuning range can be decreased by varying the generator output. In fact, zero dynamic cavity tuning is possible at the expense of power and large variation in the generator phase, i.e., the cavity can be detuned dc (κ=1) some 47 kHz.
- The technique drives the phase into a lower tuning angle that has less instability damping; see Figs. 15, F1, and F2.
- Power higher than the minimum is only needed during injection and perhaps around extraction. Storage can proceed at minimum power.
- Note that the cavity voltage is kept at the correct beam-dynamics values irrespective of the sequencing.
- There is no gain in speed by the above subterfuge. The cavity fields must be changed in either case and are limited by the cavity time constant.

73 and 503 MHz case

We forbear from including plots for the other two frequencies. Qualitatively, the same results are obtained with a likely reduction of tuning frequency by a factor of two and no tuning is required for κ=1 Estimates of any gains can be obtained by inspection of Tables II and III or a particular case can be easily calculated by the above formulae.

XIV. Single-pulse scenarios

The 4-bunch case has so far been emphasized as the more difficult and more rewarding option. Three scenarios have been described above in Section I and more fully in reference [1]. Option 1 specifies injection of a single full pulse and immediate extraction repeated each macropulse. Option 3 has a 120 μs injection period with immediate extraction 5 times in a macropulse, easiest if the extraction kicker can be cycled so rapidly. This allows $2x10^{11}$ protons in each pulse. These two scenarios can serve as a fallback position for operation while the 4-pulse case is being developed. They are far simpler than the 4-pulse case in that the ring current is lower, storage times are short, and stability does not need to be maintained after each extraction. Hence, they are deemed worthy of further elaboration.

Consider the 73-MHz case as the manifestly most difficult, but as currently favored. Here we show plots for the RF control of these two options as for the 4-pulse case in Sections XI and XIII.

Option 1

This requires $6x10^{11}$ protons accumulated in 360 μs in a single bunch. The beam dynamics are unchanged so that the required cavity voltage is the same as for the 4-pulse case. We show in Fig. 20 the equivalent of Fig. 15 and in Fig. 21 the equivalent of Figs. 18 and 19. Numbers are available in Table II.

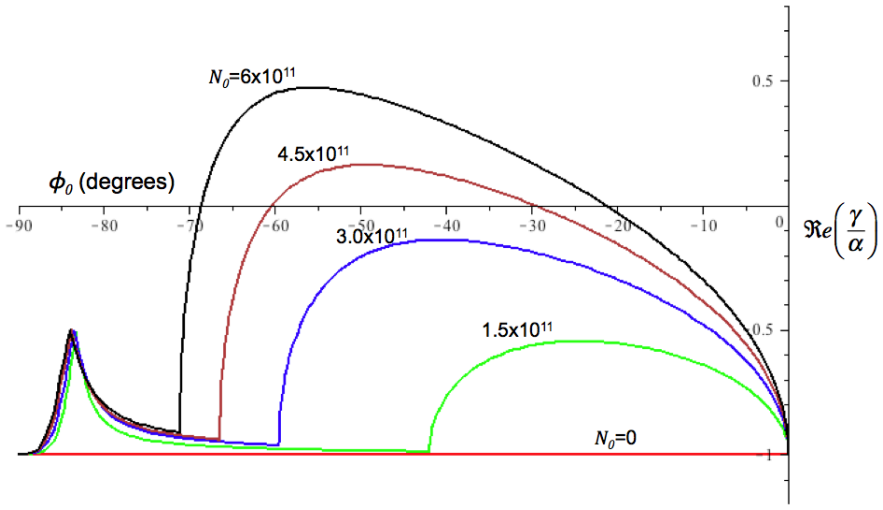

Fig. 20. Stability diagram as discussed in Section X1 *circa* Fig. 15 for the single full bunch at 73 MHz.

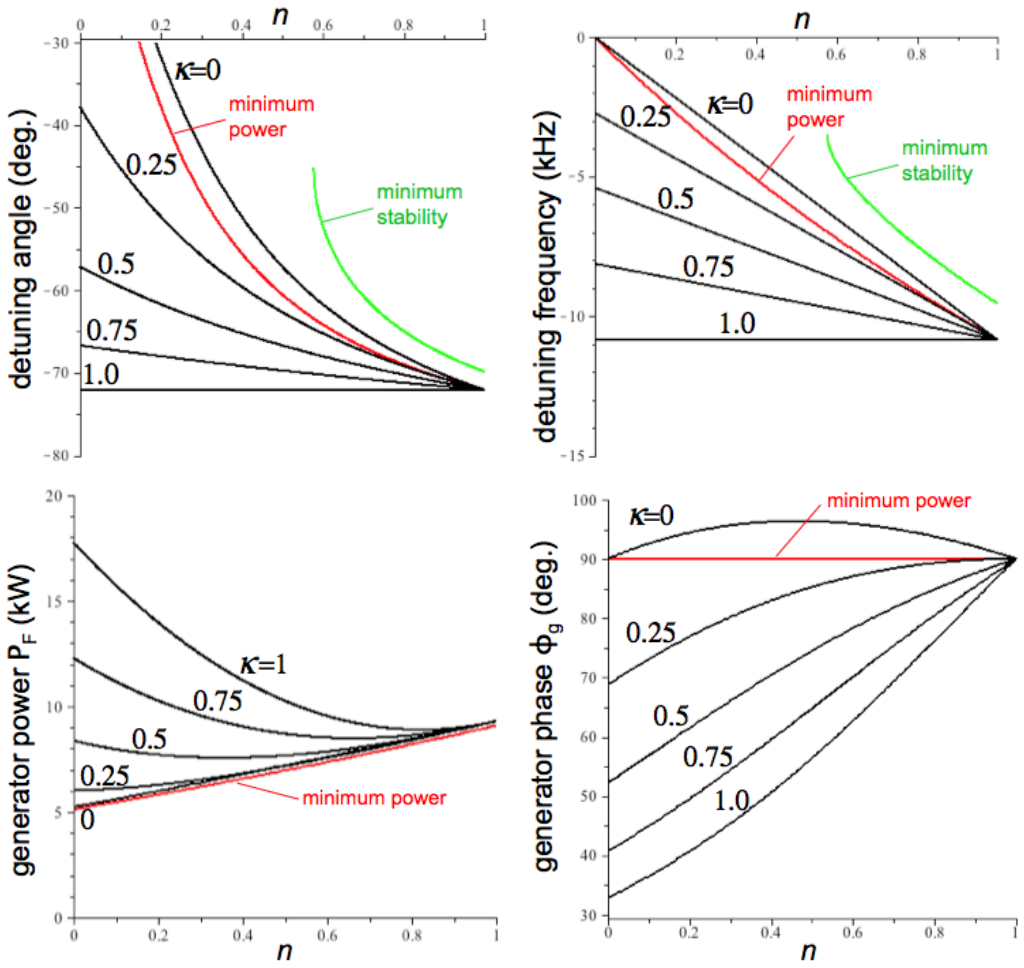

Fig. 21. Tuning diagrams as discussed in Section XIII *circa* Figs. 18 and 19 for the single full bunch at 73 MHz.

Option 3

The beam dynamics for this case (accumulation of $2x10^{11}$ particles in 333 turns) is quite different than for the full pulse. One could inject with the parameters for $6x10^{11}$ particles stopping the voltage increase at $\Delta V/3$ as in Table II, but the momentum spread is then larger than need be as well as requiring greater power and tuning. Table IV shows the beam dynamics quantities for this case as in Table I and II.

Table IV. RF system parameters for 1 pulse in the ring with $2x10^{11}$ protons

	ΔV	$V_{1\ min}$	$V_{1\ low}$	$V_{1\ good}$	$V_{storage}$	$\delta p/p$ (%)
145 MHz	0.077	0.086	0.15	0.21	0.23 to 0.29	0.25 to 0.30
73 MHz	0.019	0.021	0.040	0.062	0.059 to 0.081	0.19 to 0.22

For the 73-MHz case at this reduced charge, the equivalents of Figs. 20 and 21 are shown below in Figs. 22 and 23. Since the voltages have been reduced along with the beam current, tuning is similar to the full bunch case.

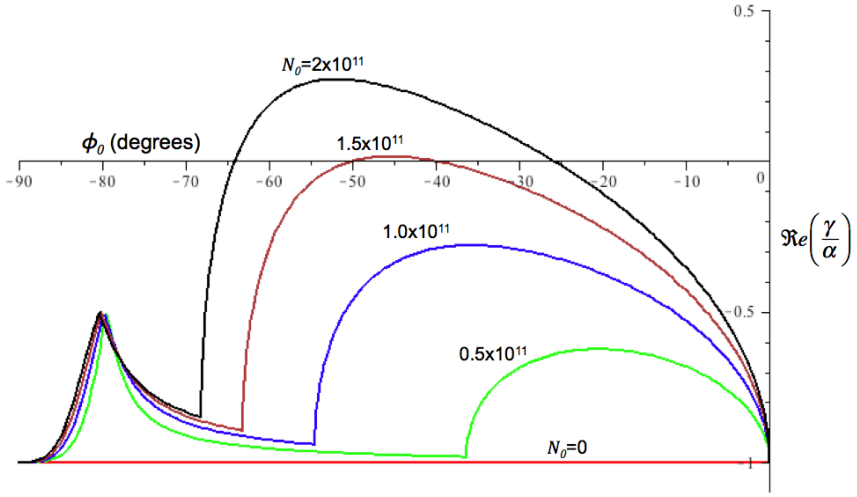

Fig. 22. Stability diagram as discussed in Section X *circa* Fig. 15 for the single bunch with $2x10^{11}$ protons at 73 MHz.

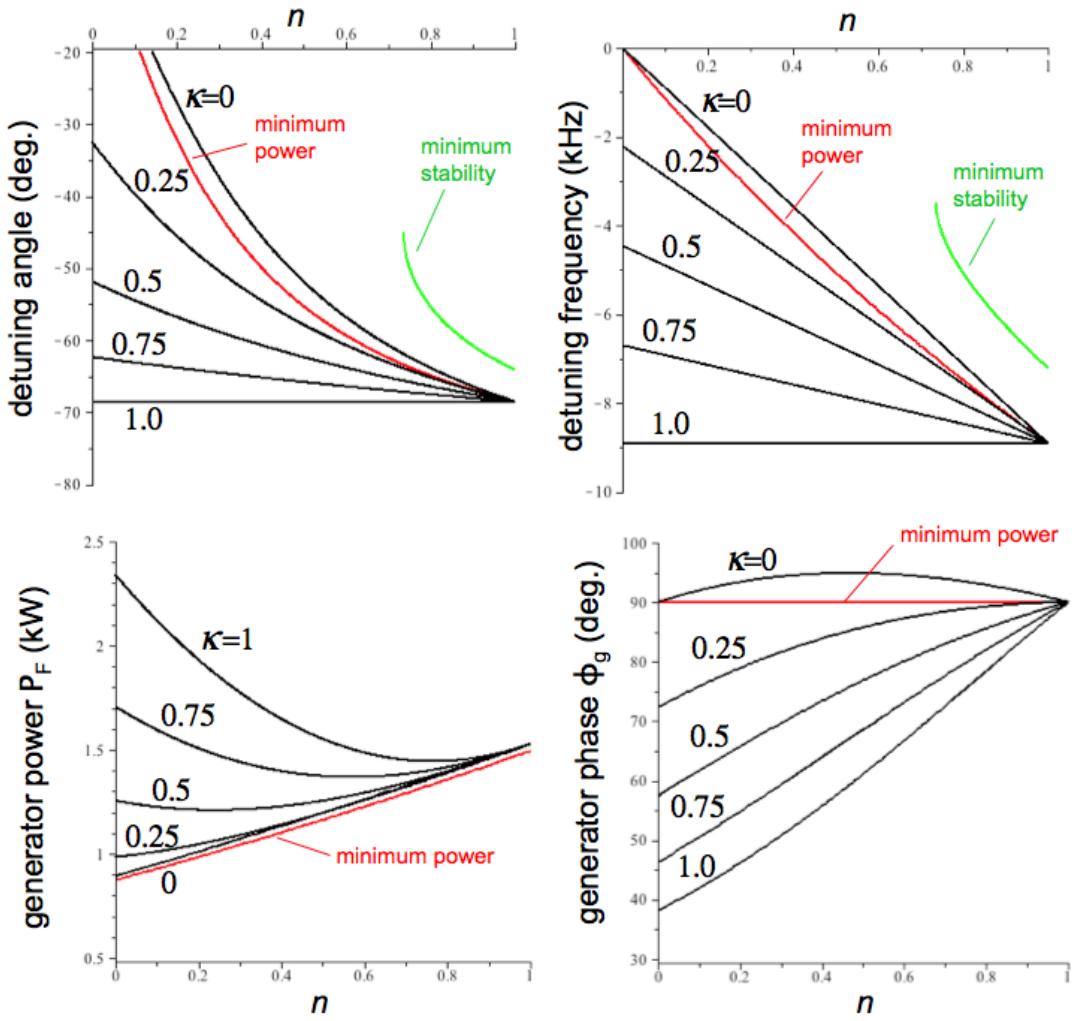

Fig. 23. Tuning diagrams as discussed in Section XII *circa* Figs. 18 and 19 for the single bunch with 2×10^{11} protons at 73 MHz.

XV. Other stability considerations

We have limited discussion here to first-order stability and beam dynamics. To augment the conclusions presented, we note that:

- Each extraction in the 4-bunch case must be accompanied by a change in the cavity (or generator) phase to prevent particle loss. Changes in the ring current during injection must also be followed by cavity tuning and voltage changes. A finite cavity response time cannot be avoided and studies are underway to develop stability criteria and tuning tactics. Hardware strategies include decreased cavity Q and lowered shunt impedance as well as appropriate feedback setups.
- Despite having a smaller Q, the lower frequency cavities have a larger time constant, detrimental to rapid tuning. Additionally, with the lower voltages, synchrotron frequencies are lower at the smaller required voltages, so that distribution of particles into symmetrical distributions is slower.

- Although fast cavity detuning can be avoided (κ=1 in Sections XIII and XIV,) dc tuning should be available to empirically accommodate realistic conditions.
- Ferrite-loaded inductances were placed in the PSR to compensate space charge forces without increasing momentum spread [14]. Because of the ferrite properties and container dimensions, a resonance at the 26th (!) harmonic with consequent beam instability was seen and removed by heating to change the ferrite properties. While the long-bunch mode works well with the inductors, the broader frequency spectrum of the short-bunch mode may make the present inductors a showstopper. Since these devices were installed to further compensate space charge (provide an inductive longitudinal force against the beam current,) it is likely that an increase in the 2.8-MHz buncher voltage would (better) replace the inductors.
- An important issue has been cited in Section VIII, regarding the effect of the long-pulse buncher on the short-pulse beam, and conversely. It seems apparent that the unused cavities cannot remain idle, but must be kept with zero gap voltage. Additionally, closer evaluation of the remainder of the ring-impedance frequency structure would be appropriate to assess the effect of undesirable resonances.
- Investigation of beam stability during injection and single-bunch extraction may change the magnitude of some of our quantities, including cavity parameters. Such a study will be presented in a future publication.

Higher-order instabilities are under study. Prominent here is the effect of bunch-to-bunch coupling for the 4-bunch case. Again, effects of the ring-impedance frequency spectrum needs further study.

It is not clear that existing codes will substantially improve the results presented here, but such studies need to be done to provide a self-consistent beam distribution. Note that preliminary runs with ESME have corroborated the magnitude of parameters cited for stable beam dynamics.

XVI. Summary and conclusions

Simply said, this work has come to conclusions about the first-order beam dynamics and RF control of the beam in a short-pulse mode, providing parameters deemed sufficiently accurate for initial hardware studies to proceed. An analytic formalism has been developed for tracking beam envelopes during injection and ranges of minimal buncher voltages have been calculated. The conditions for RF stability of a stored beam have been evaluated for the three requested modes of operation to specify needed tuning measures. Programs now exist for further exploration of parameters in the present context. Work with existing (or *ad hoc*) ring tracking codes needs to be done to verify our conclusions as does further probing into the morass of instability theory. Some assurance of correctness is had from ESME calculations and comparison of the PSR long-bunch operation with predictions, but without inclusion of the effect of beam on the RF system.

Note that injection and extraction stability, either from the RF or beam dynamics standpoints, have not been evaluated here but will be included in a further publication as necessary for a denouement of the study. Conclusions about RF storage voltages, tuning numbers, and other system parameters will likely change from this text.

Several caveats have been noted, including mode-buncher interaction, existing structures in the present ring that may be incompatible with short-bunch operation, and injection and extraction stability with the multi-pulse short-bunch mode. Other issues are included in reference [1].

References

1. Andrew J. Jason, "Short-Bunch Stacking Mode for The PSR – An Overview," LA-UR--13-20465.
2. E.g., C. Wilkinson, et al., "Comparison of beam transport simulations to measurements at the Los Alamos Proton Storage Ring" PSR Technical Note 97-015; D. H. Fitzgerald, et al., Commissioning of the Los Alamos PSR injection upgrade, Proceedings of the 1999 Particle Accelerator Conference.
3. L. M. Earley, G. P. Lawrence, J. M. Potter, "Rapidly Tuned Buncher Structure for the Los Alamos Proton Storage Ring (PSR)," IEEE Trans. Nucl. Science, NS-30, 4,1983, p3511.; L. M. Earley, H. A. Thiessen, "A high-Q ferrite tuned cavity," IEEE Trans. Nucl. Science, NS-30, 4,1983, p3460.
4. E.g., D. Horan, E. Cherbak, "High-power RF testing of a 352-MHz fast-ferrite RF cavity tuner at the Advanced Photon Source," Proceedings of the 2005 Particle Accelerator Conference.
5. AFT Microwave GmbH; http://www.aft-microwave.com/en/products/microwave-components/ferrite-based-components/fast-ferrite-tuners-i-q-modulators.html . Development of such a tuner would be a substantial effort and purchase is recommended if applicable.
6. W. R. Smythe, T. G. Brophy, "RF cavities with transversely Biased Ferrite Tuning," IEEE Trans. Nucl. Science, NS-32, 5, 1985, p. 2951. See also "Ferrite Tuning of Synchrotron Cavities," Nuclear Physics Laboratory of the University of Colorado Report NPL-987, 1984 (under LANL subcontract 9-X53-E9240-1 for LAMPF II.) Mainly ferrite evaluation, report available electronically.
7. R. K. Cooper, "Energy Acceptance Including Space Charge and Large Amplitude Synchrotron Oscillations," PSR Technical Note 058.
8. Web site for code source and overview of the latest ESME code versions may be found at http://www-ap.fnal.gov/ESME/
9. G. Waldschmidt, et al., "Higher-Order-Mode Damper Testing and Installation in the Advanced Photon Source 352-Mhz Single-Cell RF Cavities," Proceedings of the 2005 Particle Accelerator Conference.
10. R. K. Cooper, P. L. Morton, "RF stability for the PSR," PSR Technical Note 17. (Similar to a technical note by K. W. Robinson in 1964.) Further equivalent discussion on the stability criterion is given in P.B. Wilson, "Physics of High-Energy Particle Accelerators," AIP Conference Proceedings 87, p. 450. See also T.F. Wang, "Robinson Instability and Longitudinal Mode Coupling," PAC 1989 wherein except for a form factor ~1, the given instability criterion is verified using the Vlasov equation. Quadrupole and coupled bunch instabilities are also discussed by Wang.

11. Readily obtainable from http://en.wikipedia.org/wiki/Quartic_function
12. Succinctly from http://en.wikipedia.org/wiki/Routh Hurwitz_stability_criterion. For a more thorough exposition see R. Dorf, R. Bishop (2001). "Modern Control Systems," 9th Edition. Prentice Hall.
13. G. P. Lawrence, T. F. Wang, "PSR 503.125-Mhz Buncher: Generator Power and Phase for Unmatched Load Conditions," PSR Technical Note 114. (Also note an equivalent treatment in Tom Wangler's book, "RF Linear Accelerators," Wiley, 1998, Section 10.5 or P.B. Wilson, op. cit.)
14. K. Y. Ng, et al., "Recent Experience with Inductive Insert at PSR," PAC 01. Also see S.C. Breitzmann, et al., "Impedance Calculation for Ferrite Insert," PAC 2005. Basic idea by R.K. Cooper, et al., "Inductive Cavities for PSR Long Bunch Mode," PSR Technical Note 100.

Appendix A - Pulse shortening in the extraction line

Resolution of the WNR neutron pulse depends on the pulse width at the higher neutron energy range (>10 keV for the 10-ns pulse, see [1].) The 10-ns pulse provides greater intensity than the 1.5 ns pulse but at 1-MeV neutron energy has an order of magnitude poorer resolution. If sub-nanosecond bunches can be obtained by RF bunching in the extraction line, the neutron resolution will be dominated by target scattering and resolution better than 10^{-3} is achievable up to 10's of MeV. We look here at this prospect and find bunching impractical to attempt with the usual RF means. (Here we keep the full value of c in determining velocities, but retain the proton mass in eV and momentum in eV/c.) Use of a pulsed-power device is also unlikely.

Consider an uncorrelated beam with full time extent $2\Delta t$ and momentum spread $2\Delta p$ relative to the beam momentum (our Δp is usually denoted by $\delta p/p$.) The beam matrix in t,p space is given by

$$\sigma_0 = \begin{vmatrix} (\Delta t)^2 & 0 \\ 0 & (\Delta p)^2 \end{vmatrix} \qquad \text{A1)}$$

That the beam in this space is not elliptical, as A1) implies, matters little in the results that are virtually independent of the value of Δp for our range. Space charge effects are omitted from the calculation as unimportant. A linear voltage with time is assumed implying a cavity with frequency greater than twice the ring buncher. The beam is correlated early in the extraction line, with a voltage V at the beam edge, then allowed to drift longitudinally a distance $L=50\ m$ to the target. The matrices describing these steps are, respectively,-

$$R_{buncher} = \begin{vmatrix} 1 & 0 \\ -m\gamma V / p^2 \Delta t & 1 \end{vmatrix} \text{ and } R_{drift} = \begin{vmatrix} 1 & L/c\beta\gamma^2 \\ 0 & 1 \end{vmatrix}, \qquad \text{A2)}$$

where p is the beam momentum 1.46 GeV/c. Transformation to the target by $\sigma = R_{drift} R_{buncher} \sigma_0 \left(R_{drift} R_{buncher} \right)^T$ yields for the beam length squared

$$\sigma_{11} = \Delta t^2 - \frac{mVL\Delta t}{\beta c \gamma p^2} + \frac{L}{\beta c \gamma^2} \left[\frac{\left(\frac{m^2 \gamma^2 V^2}{p^4} + \Delta p^2 \right) L}{\beta c \gamma^2} - \frac{m \gamma V \Delta t}{p^2} \right] \qquad \text{A3)}$$

The bunch length at the target, from this, the square root of A3) is shown as a function of V for our three bunch lengths in Fig. A1. For each bunch length an initial momentum spread of 0.003 was used. Sub-nanosecond beams are obtained (perhaps further limited by space charge,) but the buncher voltages needed are much too high to implement. Note further that a sinusoidal buncher will have peak voltages greater than twice those of Fig. A1 to do linear bunching.

As a sanity check, we note that bunching at 750 keV to obtain a 3-micropulse intensity for WNR is readily done over 10-ns intervals at LANSCE. Use of A3) at this lower energy concludes that V~27 kV to form a WNR pulse and 18 kV to form the 201 MHz pulses, reasonable if not exact voltages.

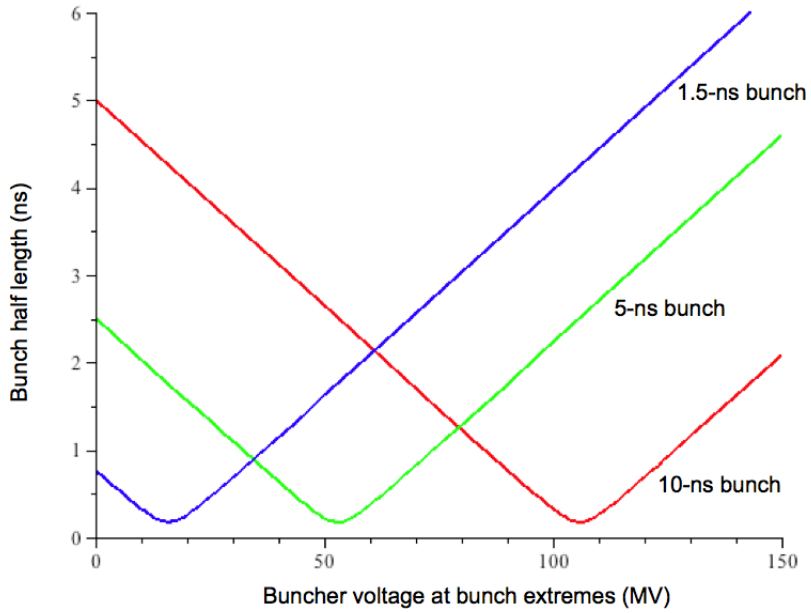

Fig. A1. Pulse length at WNR target 4 after a longitudinal drift of L=50 m vs. buncher voltage of a linear waveform measured at the bunch edges.

Appendix B. Derivation of tracking equations 13) and 14)

The first term in Eqn. 13) proceeds from the energy gain per turn $\delta E = -V_0 \sin\phi$ and the relativistic expression for the change in the relative momentum

$$\Delta\left(\frac{\delta p}{p}\right) = \frac{1}{\beta^2}\frac{\delta E}{E_{total}} = \frac{1}{\beta^2}\frac{\delta E}{\gamma m_p}. \qquad \text{B1)}$$

The second term is derived from the expression for the electric field Eqn. 2) with the assumed parabolic distribution of charge along the z axis

$$\lambda = \frac{3N}{4z_m}\left(1-\frac{z^2}{z_m^2}\right), \qquad \text{B2)}$$

where z_m is the maximum extent of the distribution. Using $z=R\phi/h$, the electric field becomes

$$E_z = \frac{3\pi g r_p m_p h^2 N}{\gamma^2 R^2 \phi_m^2} \qquad \text{B3)}$$

The change in momentum for one turn with period T is

$$\Delta(\delta p) = E_z T = \frac{2\pi R}{\beta} E_z. \qquad \text{B4)}$$

Finally dividing by the momentum $m_p\beta\gamma$, the second term is verified.

Eqn. 14) comes directly from the definition of the ring slippage factor for each turn

$$\Delta T = \eta T \frac{\delta p}{p} \qquad \text{B5)}$$

Using the relations $T = \frac{2\pi R}{\beta}$ and $\Delta\phi = -\frac{h\beta}{R}\Delta T$, Eqn. 14) is obtained. Alternatively, integrate Eqn. 7.

Appendix C Field outside the bunch

To our approximations, the field along the axis outside the bunch in the beam tube varies inversely as the distance from the bunch center. This was easily added as a piecewise continuous function. Otherwise, particles that move outside the desired bunch width will be further repelled, in violation of the model of a given bunch width. This addition makes little difference in the stable voltages. To illustrate the fields involved, Fig. A1 shows the momentum kick given per turn by the buncher and space charge for the case illustrated in Fig. 10 at $3\text{x}10^{11}$ particles/pulse.

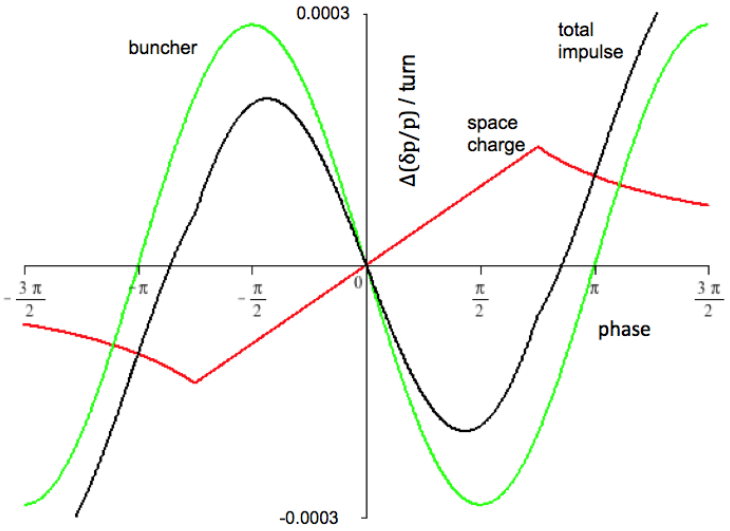

Fig. B1. Impulse given by buncher (green), by space charge (red), and by combined buncher and space-charge (black) terms per turn for the case of Fig. 10.

Appendix D Beam transformation around the ring

The beam pulse passes through the buncher where it is influenced by the first term in Eqn. 13). Unlike the assertion of Eqns. 13) and 14), the space-charge forces influence the beam in traveling around the ring and will give a somewhat different result for the change in momentum and phase. To assess this, consider dividing the course through the ring into n divisions. We then have for each division

$$\Delta\phi = -\frac{2\pi h\eta}{n}\frac{\delta p}{p} \equiv \frac{A}{n}\frac{\delta p}{p}$$
$$\Delta\left(\frac{\delta p}{p}\right) = \frac{3\pi g r_p h^2 N}{n\beta^2\gamma^3 R\phi_m^3}\phi \equiv \frac{B}{n}\phi \qquad \text{C1)}$$

defining the elements of the matrix

$$\mathbf{R} = \begin{bmatrix} 1 & \frac{A}{n} \\ \frac{B}{n} & 1 \end{bmatrix}^n \text{ operating on the vector } \begin{bmatrix} \phi \\ \frac{\delta p}{p} \end{bmatrix} \qquad \text{C2)}$$

to obtain the changes in the vector for one ring turn. Expanding **R** and taking the limit

$$\lim_{n\to\infty}\mathbf{R} = \begin{bmatrix} \cosh\sqrt{AB} & \sqrt{\frac{A}{B}}\sinh\sqrt{AB} \\ \sqrt{\frac{B}{A}}\sinh\sqrt{AB} & \cosh\sqrt{AB} \end{bmatrix} \qquad \text{C3)}$$

This then provides the beam transformation around the ring. For small enough values of *AB* this reduces to 13) and 14). To see the effect on our calculation, evaluate C3) for the 503 MHz case (the cavity voltage doesn't matter here.)

$$\mathbf{R}_{\infty} = \begin{bmatrix} 1.027 & 225.59 \\ 0.000242 & 1.027 \end{bmatrix} \qquad \text{C4)}$$

whereas without the correction (n=1) the matrix is

$$\mathbf{R}_{1} = \begin{bmatrix} 1 & 223.6 \\ 0.000239 & 1 \end{bmatrix} \qquad \text{C5)}$$

thus having small effect on the calculation results.

Appendix E Beam-injection-tracking examples

We follow the 145-MHz injection tracking from voltages below stability to well above in E1 to E3 below in each case with injection according to Eqn. 15) proceeding in 500 turns. E4 tracks the PSR long-bunch mode for allegedly stable settings with injection over 1738 turns. In each case ϕ_c was set at $\pi/2$ to determine ΔV by Eqn. 17). The left-hand plot shows the motion in the bucket for a particle starting its motion at $-3\pi/4$ and $-3\pi/8$, the center plot the momentum kick/turn, and the right-hand plots the change in phase/turn.

E1. Storage voltage V_c set at minimum voltage 0.24 MV from Eqn. 9) with V_1 calculated from Eqn. 19). 0.128 MV. The storage voltage identically equals the sum of V_1 (Eqn. 19) and ΔV (Eqn. 17) as calculated for this case, i.e. the static total Eqn. 9). As expected, unstable motion shows the phase monotonically increasing with turn number. The center and right-hand plots are certainly not accurate since the space-charge model does not correctly describe the situation, but are merely an indication of particles leaving the bunch and show qualitatively the expected behavior for particles in the continuum.

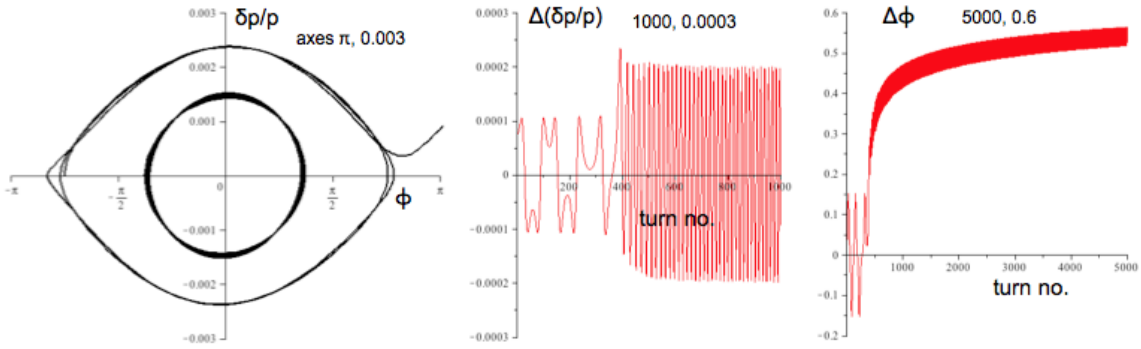

E2. V_1 set at simulation minimum 0.235 MV ($V_{1\,low}$ in Table I) and ΔV at the calculated value 0.115 MV from 17). Motion is stable for >10,000 turns but becomes unstable at $V_1 \leq 0.232$ MV. Clearly a "threshold" but unconvincing since the calculation requires a definite bunch length.

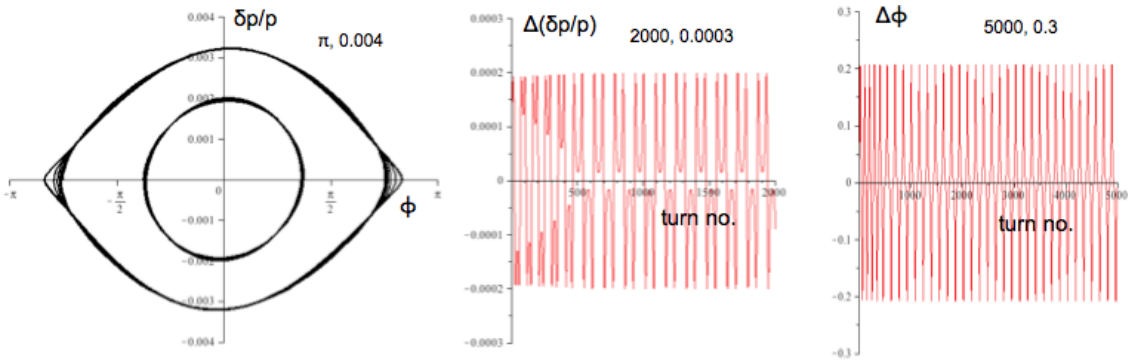

E3. V_1 set at guess 0.31 for "small-enough" excursions at bunch ends. (V_{1good} in Table I)

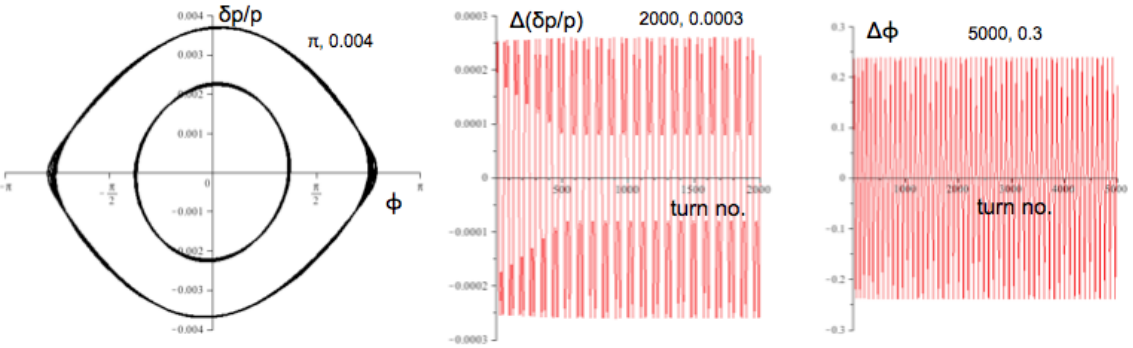

E4. V_1 set at 0.015 MV, ΔV calculated 0.0057, storage voltage 0.0207 MV for the PSR long-bunch mode. ($V_{1\ good}$ in Table I)

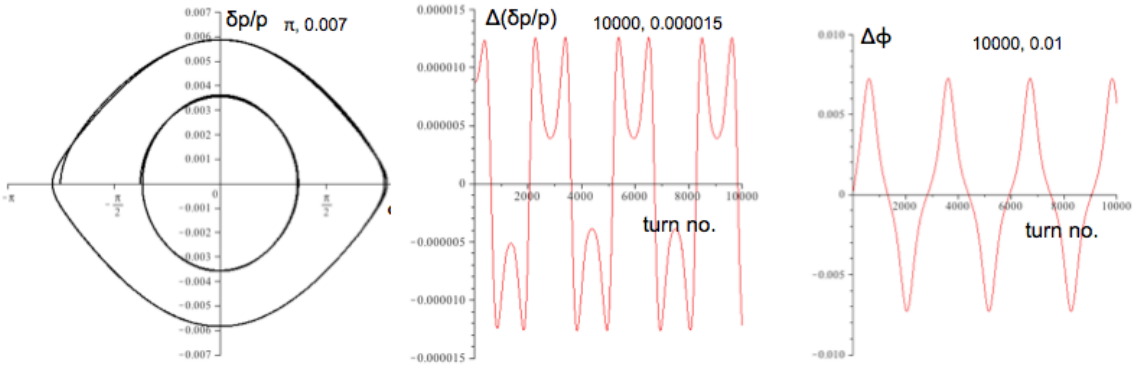

Appendix F Damping-time plots for 503 and 73 MHz

Plots of damping time for the voltages and particle numbers as explained in Section X. Although the plot of the roots' imaginary parts are not shown, such plots are much like Fig. 16, mainly showing that the motion is critically damped for phase greater than given by Eqn. 26), the minimum generator power. The result for 73 MHz looks unfavorable but the cavity parameters used may be unrealistic.

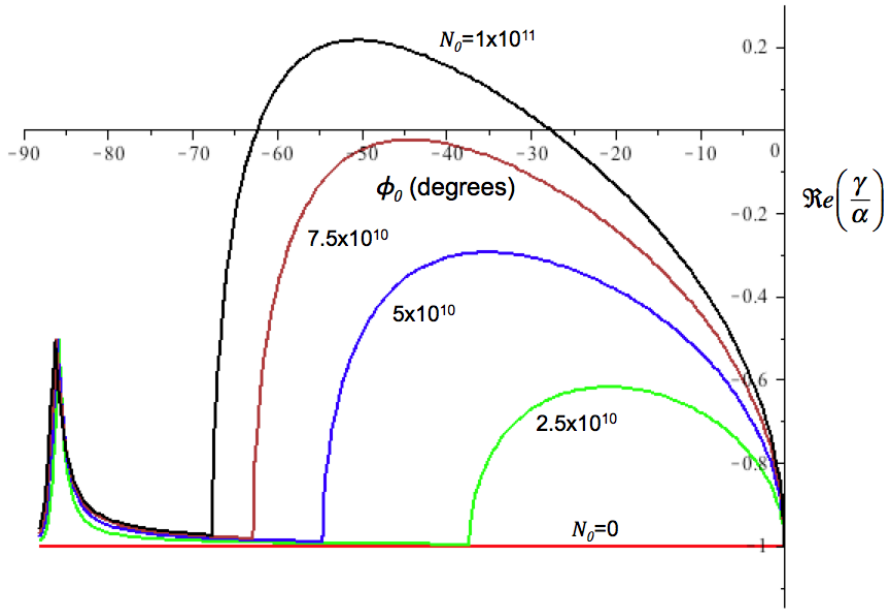

Fig. F1. Plot of damping time/cavity response time versus phase ϕ_0 as a function of number of particles/pulse for 4 pulses in the ring and a buncher frequency of 503 MHz.

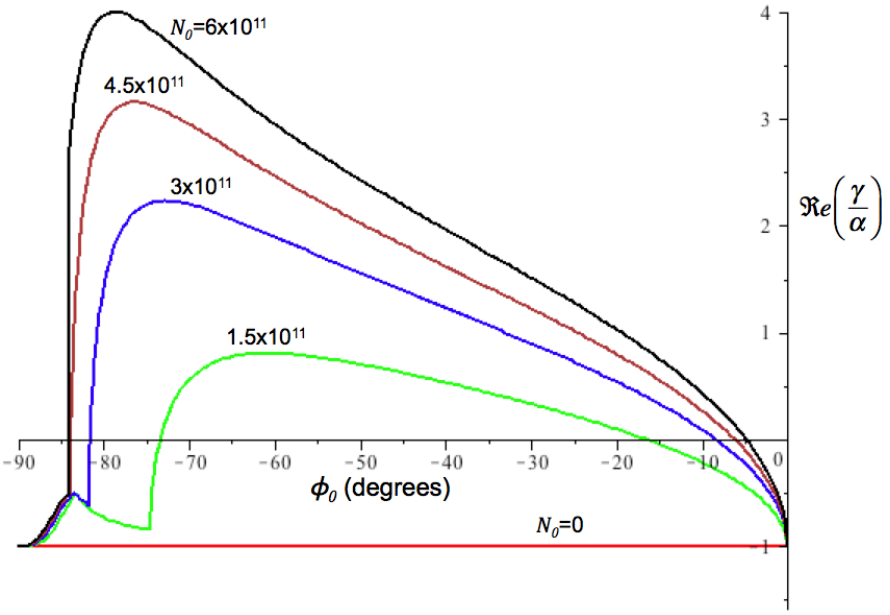

Fig. F2. Plot of damping time/cavity response time versus phase ϕ_0 as a function of number of particles/pulse for 4 pulses in the ring and a buncher frequency of 73 MHz.

Dated postscript

After further work on the injection and stability issues cited, the following document were issued concerning RF control and beam-dynamics interface during injection and extraction.

Andrew. J. Jason, “Stability and parameter determination for injection and extraction in the PSR short-bunch mode,” LA-UR-13-20496.